

The Third Dimension: Crater Depths from the Apollo Era to the Present

Kurt Allen Fisher, member Salt Lake Astronomical Society

Submitted 7 January 2007 to *Selenology Today*

Review comments received 11 Feb. 2007, corrections submitted 14 Feb. 2007

Further corrections and additions submitted 23 Feb. 2007

**Deleted: ¶
Review**

Deleted: ruary

Abstract: A digitized table of 1,866 higher accuracy crater depths from the Apollo era associated with U.S. Geological Survey Gazetteer of Planetary Nomenclature (GPN) positions is provided in the supplementary materials. 86% of the craters in table have diameters less than 20km and 83% have depths of less than 2km. Existing catalogues of crater depths and feature heights have a 5 to 10% variation for craters with diameters larger than 10 km and up to 30% for craters less than 10km. Developments increasing the accuracy of techniques used to measure the height of lunar topography are reviewed from the Apollo era to the present, including lunar control point networks, digital elevation models from stereophotography and laser altimetry, Doppler radar interferometry, photoclinometry, and shadow measurements. Even with technological developments, advances in consumer astrophotography and computing provide an opportunity for amateurs to make continuing contributions to lunar topography studies.

1. Introduction

“How big and how deep is that hole?” are common questions received by lunar observers from the general public. Yet answering that question with a reasonable degree of scientific certainty is more difficult than appears on initial inspection. Lunar topography is a statistical science. There is no absolute true height of Mons Piton or depth and diameter for Bessel H. There are statistical estimates for those values which have an inherent uncertainty.

A few standard references that are consulted for the depths of larger named lunar craters include Westfall's compilation of crater diameter and depth catalogues and Viscardy's Earth-based shadow measurements (Westfall 2000, Viscardy 1985). The GPN is another well-known standard reference for crater diameters which incorporates earlier work by Andersson and Whitaker. ([USGS 2006b](#), [Andersson and Whitaker 1982](#)) Although Andersson and Whitaker (and the GPN) contain high-accuracy crater diameters, the catalogue rounds crater diameters to the nearest kilometer. The catalogue includes no crater depths or feature heights.

When the depth or diameter of archetypal features are compared between catalogues – such as the diameter of Tycho or the height of its central peak – variations of greater than 10% can be found between different sources :

Researcher	Diameter (km)	Depth (km)	Central peak height (km)
US Air Force, NASA and ACIC LAC 112 1967		4.46	1.56-2.19
Wood 1973			2.26
Pike 1976	85	4.6	
Andersson and Whitaker 1982	102		
Viscardy 1985	88	4.8	
Margot et al. 1999a	85	4.7	2.4

Table 1 – Measurements of the diameter and depth of Tycho and its central peak

Less well known are a series of high-accuracy crater depth and feature height data made during the Apollo era by Arthur, Pike and Elachi with respect to smaller satellite feature craters. ([Arthur 1974](#), [Elachi *et al.* 1976](#), [Pike 1976](#), and [Wood 1973](#)). These researchers based their work in part on oblique stereophotography from the Lunar Orbiter missions of the 1960s and Apollo 15, 16 and 17 Command Modules.

Thirty years later their work still represents some of the highest accuracy topography data available on the lunar nearside lunar surface:

Despite the fact that the Moon has been visited by six manned missions and a multitude of unmanned spacecraft, its surface is far from being completely explored. . . . [T]he best available set of spacecraft images globally covering the lunar surface, taken under low to moderate illumination angles and thus revealing the relief of the lunar surface, is still that obtained during the Lunar Orbiter programme in the mid-1960s. [[Lena 2006](#).]

Part of higher accuracy Apollo era catalogues of Arthur, Elachi *et al.*, Pike and Wood have been associated here with standard GPN feature names. Those crater depth and diameter measurements, mostly for smaller satellite features, are digitized in the supplementary materials. While answering the questions “How big and how deep is that hole?”, a review of Apollo era topography studies also tells an interesting story of a portion of that exploration’s history.

This historical review is intended as a continuation of [Davis 1997](#) for the period 1996 through 2006.

2. Crater depth and diameter measurements during the Apollo Era

2.1. 1500 meter accuracy - Lunar Aeronautical Chart (LAC) measurements from Earth based telescopes

In 1960, D.W.G. Arthur, E. Moore, J.W. Tapscott and E.A. Whitaker (Gerard Kuiper ed.) published the *Photographic Lunar Atlas*, a compilation of lunar terrain photographs from the best telescopes in the world ([St. Clair et al 1979](#)). Companion volumes were published: the *Orthographic Atlas of the Moon* in 1961 and the *Rectified Lunar Atlas* in 1962 ([Kuiper 1961](#), [Whitaker, Kuiper and Hartmann 1963](#), [St. Clair et al 1979](#)). Rectification removes foreshortening and displays features on the lunar surface in their correct geometrical relationship.

The Army Corps of Engineers' 1964 Topographic Lunar Map represented the first Apollo era attempt to create a nearside lunar elevation map - now commonly called digital elevation maps or "DEMs" - from which the relative altitudes of features could be ascertained ([Army Map Service 1964](#)). The 1964 [Topographic Lunar Map](#) (TLM) has a vertical resolution of 1,000 meters based on a sphere of 1737.988 kilometers. All elevations were based on a low-nearside zero elevation point on the floor of Aristarchus which was measured to be about 7,000 meters below the floor of the Möstling A ([Schirmerman, U.S. Defense Mapping Agency 1973](#) at Sec. 4.1.7). Recent values for these elevations are 1735.96 kilometers for Aristarchus (ULCN 2005 Control point BA4127C) and 1737.465 (ULCN 2005 Control point 8) for Möstling A – a relative elevation difference of about 2 kilometers ([Archinal et al. 2006b](#)). The Topographic Lunar Map was developed from stereo-projection of plates taken at the Paris Observatory between 1896 and 1907 at different libration angles. No uncertainty statement concerning elevations is provided on the TLMs.



Figure 1 - [Topographic Lunar Map 1964](#) (Excerpt for the region surrounding Aristoteles, Eudoxus and Bürg)

In the early 1960s, the Aeronautical Chart and Information Center of the U.S. Air Force published the [Lunar Aeronautical Chart \(LAC\) series](#) as navigational aids for the Apollo missions. St. Clair provides a retrospective of the U.S. Defense Mapping Agency (USDMA) LAC program and other USDMA Apollo charting efforts ([St. Clair *et al* 1979](#)).

The LAC charts were based in part on photocomparator measurements of Pic du Midi Observatory telescopic photographs of the Moon ([Arthur 1974, p. 116](#)). The stated uncertainty is printed on each chart. For example, [LAC 112](#) for the Tycho region reads: “The probable error of the localized relative elevations is 100 meters in the vicinity of the center of the moon with the magnitude increasing to 300 meters at 70° from the center due to foreshortening.”

There is a systematic bias of up to 1500 meters present in the original LAC charts (C.A. Wood, 2006 personal communication). The systematic error in the LAC charts is traceable to the Pic du Midi Observatory negatives ([Arthur 1974, p. 117](#)).

The elevation of lunar features can be stated in either relative or absolute terms. In a table of relative feature heights, for example the crater depth table in the supplementary materials, only provides information the relative distance between the mean rim crest of a crater and its mean floor. Absolute elevations are expressed with respect to a common base elevation and are more useful. For the Moon a typical base elevation is 1,739km. Charts based on absolute elevations are more useful. Absolute elevation charts provide not only the height of the central peak of crater Tycho relative to its floor, but also inform the users of whether the central peak of Tycho is in absolute terms higher or lower than the central peak of Arzachel.

To convert relative elevation data on a series of images or charts to absolute elevations, a series of control points – locations whose three dimensional positions are well-established – must be used to register each image or chart into a common coordinate system. The control point network used to align a series of images or charts into a common system also has its own uncertainty, separate from relative elevation measurements on an individual chart or image.

Charts in the LAC series are a hybrid of relative and absolute elevation methods. Most of the measurements on the chart series are relative, *e.g.* the central peak of Tycho on [LAC 112](#) is 1.56km above the crater floor in one direction and 2.2 km above the floor in another direction. Control points with absolute elevations are plotted separately, *e.g.* the floor of the satellite feature Kaiser C (S36.3, E9.7, dia. 12.45km) shown on [LAC 112](#) is listed at an absolute elevation at a lunar radius of 1,739.1km; the rim to floor depth is 1.35km, and the rim to surrounding plane height is 0.54m. A later higher accuracy depth measurement, listed in the supplementary table, shows Kaiser C's depth at 2.52km. In the ULCN 1994, discussed below, Kaiser C is listed with an absolute elevation at a lunar radius of 1,737.2 km.

The Aeronautical Chart and Information Center (ACIC) Selenodetic System of 1965 (revised 1969) provided a network of 150 control points that supported the absolute elevations listed on the LAC series ([St. Clair et al 1979](#)). The ACIC of 1965 was prepared from Earth-based telescope observations and had a horizontal accuracy of 500 to 2000 meters ([St. Clair et al 1979](#)).

LAC topographic crater measurements and control points are illustrated in the following excerpt from [LAC 26](#) for the crater Eudoxus. A control point in the floor of crater Eudoxus D at elevation-radius 1,739.4 km is highlighted by the red box.



Figure 2 - [Lunar Aeronautical Chart 26](#) (Excerpt for the region surrounding Eudoxus)

During the early 1960s, the United States Geologic Survey (USGS) under the direction of Eugene Shoemaker prepared the [Geologic Atlas of the Moon](#), a 13-color geologic chart series that parallels the LAC series (Cherrington 1984 at 45).

2.2 100 meter vertical accuracy - the Lunar Orbiter IV image measurements

By 1965, D.W.G. Arthur concluded that unexplained abnormally large errors in earth based telescope measurements could not give useful data on the diameters and relative depths of smaller craters ([Arthur 1974, p. 117](#)). 1966 through 1967 brought the first systematic remote satellite imaging of the Moon by the Lunar Orbiter I-V series. Arthur undertook measurement of smaller craters based on Lunar Orbiter IV images to a two-significant digit precision. During 1969 through 1973, Charles Wood joined the Lunar and Planetary Laboratory, University of Arizona, working under D.W.G. Arthur, and supervised the higher precision measurement of the diameter and relative depth of about 7,000 nearside craters using Lunar Orbiter IV images (Wood 1974, unpublished, [Wood 2004](#)). Arthur published approximately 1,900 of Wood's measurements including crater size, crater depth and Arthur crater class ([Arthur 1974](#)). Arthur described prosecution of the work as follows:

The work was performed by student assistants under the immediate supervision of Charles A. Wood. I set out the general guide lines of the work and formulated the special mathematics required for the reduction. Occasional visits were sufficient to exercise general supervision and to deal with special problems. . . . [Arthur found that] [t]he smaller lunar craters are indeed smaller than indicated by the ACIC [LAC] determinations and those of Baldwin [[Arthur 1974, p. 117](#)].

With respect to approximately 1,900 craters that are a subset of Wood's 7,000 plus nearside measurements, Arthur noted that his 1974 catalogue was restricted to those craters that have higher confidence measurements:

The catalog of this paper is much briefer [than Wood's full catalogue], is restricted to those craters which were included in the measures, and is quite differently arranged. The two catalogs, however, contain the same depth results, except where I have suppressed heights relating to large irregular objects. Note that the measures were restricted to those craters in which the lower end of the shadow (the tip) fell close to the center of the interior of the crater [[Arthur \(1974\), p. 118](#)].

Arthur stated measurement uncertainty for the reduced catalogue at ± 100 meters for large complex craters and ± 25 to 50 meters for smaller simple craters ([Arthur 1974, p. 121](#)). Although the original Wood catalogue covers the entire nearside, in the smaller higher confidence catalogue, Arthur limited crater depth data to a spherical square bounded the north-south 45° and east-west 45° selenographic meridians ([Arthur 1974, p. 120](#)) as shown in Figure 3.

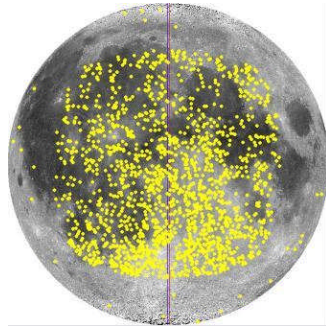


Figure 3 - Distribution of Arthur 1974 crater depths presented in the supplemental materials. Image - LTVT

1610 diameter and relative depth measurements from Arthur's catalogue are digitized in the supplementary material table. The remaining crater depths either could not be associated with GPN names or did not meet the inclusion criterion discussed in the Appendix.

Arthur also developed a new method for reducing feature heights and depths from shadows.

In the classical reduction method derived from Earth based observations, the geometry of Earth, Sun and Moon relationship are determined from a lunar ephemeris, the angular size of the hypotenuse shadow is determined using a reticule, microfilament or lunar photograph and the linear height of the feature is estimated (Chervel and Legrand 1994, [Kopal 1962](#), MacDonald 1931). Jamieson's DOS lunar reduction tool software – which is based on MacDonald's classical mathematical algorithm for shadow measurement -historically has been used lessen the burden of reduction of Earth-based shadow measurements ([Davis 1997](#), [Jamieson 1997](#), [Jamieson 1993](#)).

In Arthur's reduction method for Lunar Orbiter images, an initial guess of the linear size on the Moon of the hypotenuse shadow is made (for example, from a rough chart take-off), the order of computation is reversed and an estimate of the photographic linear size of the hypotenuse shadow and the height of the feature are made. Iteration is used to minimize the root mean square error of the estimate of the size of hypotenuse shadow on the photographic image ([Arthur 1974, p. 118-120](#)). This also yields a final estimate of the height or depth of the feature.

Wood also estimated the heights of approximately 37 central peaks of craters ([Wood 1973](#)).

2.3 100meter vertical accuracy - Lunar Topographic Orthophotomap (LTO) series

High-resolution photography from the Command Module of the last three Apollo missions - Apollos 15, 16 and 17 - launched another phase in lunar cartography. The images for the nearside roughly correspond to a "V" shaped band running between N20° and S20° selenographic latitudes shown in Figure 4.

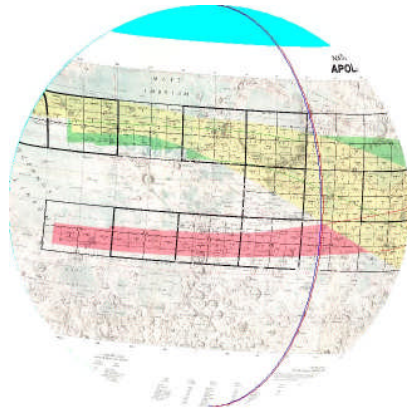


Figure 4 - [NASA 1980. Lunar Topographic Orthophotomap \(LTO\) Series Apollo Photo and Map Index Map](#) fitted to lunar globe. Image - LTVT

Stereographic photomaps were prepared by the U.S. Defense Mapping Agency from the Apollo images - the [NASA Lunar Topographic Orthophotomap \(LTO\) series](#) - with an unprecedented depth accuracy stated by Schirmerman: "The evaluated horizontal and vertical accuracy of subject series at 90% probability generally ranges from 160-500 meters and 30-115 meters respectively . . . [[Schirmerman, U.S. Defense Mapping Agency 1973.](#)]" A sample excerpt for a 100-meter accuracy LTO map for the Apollo 15 - Mt. Hadley landing site is shown in Figure 5.

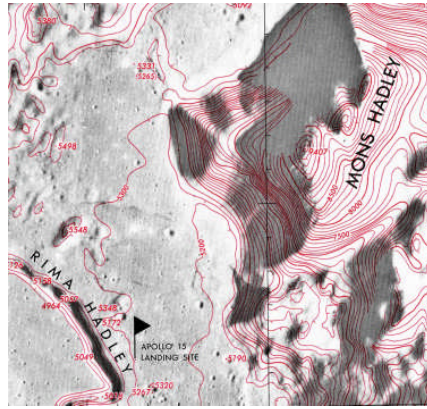


Figure 5 - [U.S. Defense Mapping Agency 1975. Map LTO-41B4](#) (Excerpt)

Individual maps in the series contain additional accuracy statements. [Map LTO-41B4](#) states a 90% accuracy of 176 horizontal meters and a vertical accuracy of ± 41 meters. The LTO series are available by internet download from the [Lunar and Planetary Institute](#).

Although highly accurate, the LTO series covers less than 20% of the Moon's near and farside surface ([Archinal *et al.* 2005](#)).

2.4 20-50 meter accuracy - Lunar Topophotomap (LTP) series

Micromaps of specific lunar features from the Apollo stereograms - the [NASA Lunar Topophotomap \(TPM\) series](#) - were prepared by the U.S. Defense Mapping Agency with 20 meter contour lines. The uncertainty for each map is printed in its legend. Typical is map [LTP 41B4S1\(50\)](#) for the Apollo 15 Mt. Hadley landing site which states a horizontal accuracy of 61 meters and a vertical accuracy of ± 20 meters.

The LTO and TPM series represent a major advancement over the LAC series in lunar topographic charting. All elevations on the LTO and TPM series are absolute with respect to common base elevation of 1,730km. For example, on map [LTO-41B4](#), crater Hadley C is shown as having floor at an elevation of 4,230 meters, a rim at 5,500 meters and the surrounding plain at 5,100 meters. This implies a crater depth of 1,270 meters. The table in the supplementary materials lists Hadley C with a depth of 1,160 meters.

The Apollo 15 Control System provided a network of 5,629 control points based on Apollo 17 LIDAR data and Apollo 15, 16 and 17 stereophotographs ([St. Clair et al 1979](#), [Archinal et al. 2005](#)).

2.5. Pike's crater depth measurements from the LTO and LTP series

Pike used a combination of measurements from Arthur, lunar topographic orthomaps, Lunar IV imagery and Apollo 15 through 17 panoramic picture cameras to measure numerous dimensions for 484 craters and other features on the near side Moon ([Pike 1976](#)). The table presented in the supplementary materials extracts 212 of Pike's crater measurements for diameter and depth that easily could be associated with GPN listed features. The remaining measurements in Pike's catalogue are for unnamed craters, non-crater features, craters with no corresponding GPN entry or craters that did not meet the inclusion criterion described in the Appendix. Pike's catalogue also indicates whether a crater has a central peak, but does not record the height of the central peak. Figure 6 shows the distribution of part of Pike's and Elachi *et al*'s catalogues (discussed below) on the nearside. Compare to Figure 4, above.

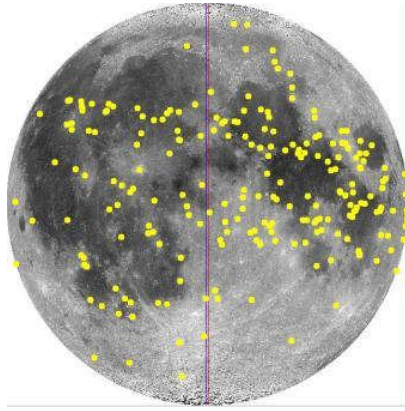


Figure 6 – Distribution of features digitized from [Pike 1976](#) and [Elachi *et al.* 1976](#). Image - LTVT

2.6. 25 meter accuracy - Apollo 17 radar altimeter and Elachi *et al.* depth measurements

Elachi *et al.* reported the results of a radar altimeter that was attached to the Apollo 17 Command Module - the Apollo Lunar Sounder Experiment (ALSE) ([Elachi *et al.* 1976](#)). (The lead researcher, Dr. Charles Elachi, is presently a director of the Jet Propulsion Laboratory and a leader on the Cassini Titan radar team ([JPL 2006](#)).) The ALSE provided a continuous 30 kilometer wide swath of altimeter readings, including profiles for large maria like Crisium, Tranquilitatis and Serenitatis. Elachi *et al.* also reported high precision 25 meter accuracy crater diameters and depths for 16 craters. Ten of these 16 craters could be easily matched to the GPN and seven are included in the supplementary material table. Smaller crater measurements cover features in [Arthur 1974](#).

2.7. Relationships between crater dimensions

2.7.1. Crater depth to crater diameter relationships

Among the features measured by Pike, included:

Rim diameter - average rim-crest to rim-crest diameter;

Depth - vertical distance from the rim diameter elevation to the crater's central low point;

Floor diameter - diameter of the floor to terraced or slumped walls;

Rim flank - horizontal distance from rim crest to elevation of the level of surrounding plain;

Rim height - vertical distance between rim crest to elevation of the level of surrounding plain;

Apparent diameter - the diameter of the crater at elevation of the level of surrounding plain; and,

Apparent depth - vertical distance from the apparent diameter elevation to the crater's central low point ([Pike 1976](#), *id.* at Fig. 1, [Pike 1977](#)).

In *The Lunar Sourcebook*, Heiken *et al.* summarizes empirical relationships found from the Apollo era data ([Heiken *et al.* 1991](#) at Table 4.1). Such empirical mathematical relationships are all in the form of $y = a * Drc^b$ - where a and b are coefficients and “Drc” is the rim to rim diameter of the crater.

Pike found empirical relationships between crater depth and diameter based on 170 small craters less than 15km in diameter ([Pike 1974](#)). Elachi *et al.* also plotted small crater depths to their diameters, finding that for his small sample of craters less than 30 kilometers in diameter, the ratio of the crater depth was constant at 0.2 ([Elachi et al. 1976](#), *id.* at Fig. 2). For large craters, Pike also found an empirical relationship of rim-to-rim crest to depth of about $Drc^{0.3}$. Pike did further follow-up work on the crater diameter to depth relationships based on apparent crater volumes as opposed to rim-to-rim crest diameters ([Pike 1977](#)). These diameter to depth relationships are summarized in the following table and figures.

Researcher	Applies to crater dia. km	N crater	Equation
Elachi et al. 1976	< 15km	16	$Dp=0.2*Drc$
Pike 1974	< 15km	171	$Dp=0.196*(Drc^{1.010})$
Pike 1974	> 12 - < 275km	33	$Dp=1.044*(Drc^{0.301})$

Table 2 - Crater diameter to depth relationships

A plot of the ratios of 1,905 crater depths to diameters – an expanded set of craters from the list in the supplemental materials– is shown in Figure 7 and illustrates Elachi *et al.*'s small crater depth to diameter ratio of $0.2*Drc$. In Figure 7, the trend line is fitted to 11 of 16 of Elachi *et al.*'s craters.

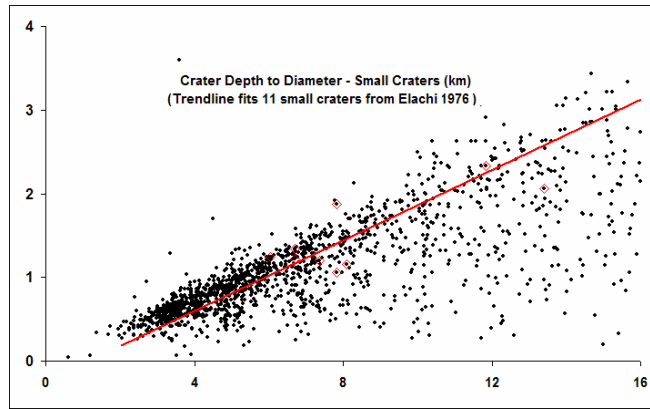


Figure 7 - Small crater (<15km) depth to diameter relationship

Pike's large crater depth to diameter relationship is illustrated in Figure 8 by crater diameter for 1,905 nearside craters. To improve graphic clarity, Figure 8 plots the reciprocal of Pike's large crater relationship – the ratio of the crater depth to diameter to crater diameter.

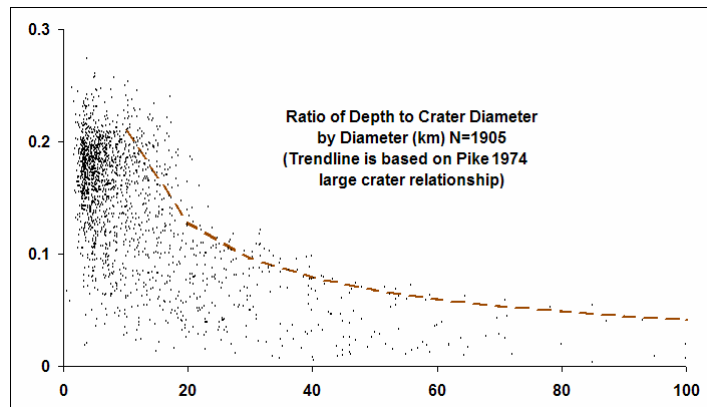


Figure 8 - Large crater (>12km) depth to diameter relationship

Wood and Andersson examined 2,589 fresh Copernican nearside craters in more detail ([Wood and Andersson 1978](#)). They defined morphology classes for this group of young craters into statistical archetypes represented by Albategnius C, Biot, Sosigenes, Triesnecker, and Tycho. Wood and Andersson better defined equations statistically relating the diameters of craters in each morphological subtype to their depths and central peak heights. They reconciled differences between crater diameter to depth relationships found in their larger crater sample and in Pike's previous work based on differences between subpopulations of highland and mare craters.

2.7.2. Central peak height to crater diameter relationships

Hale and Head measured the characteristics of crater diameter, rim crest height and central peak height for 90 nearside and 85 farside craters from the LTO map series for craters larger than 17 km in diameter ([Hale and Head 1979](#)). This was part of a continuing series of studies following up on [Wood 1973](#). They proposed equations to relate rim crest crater diameters and the crater floor width to the height of the crater's central peak. Hale and Head did not publish a catalogue of craters and central peak heights on which they based their conclusions. Hale and Grieve performed a similar analysis based on digitized LTO maps and the volumes, not diameters, of craters ([Hale and Grieve 1982](#)). The empirical relationship between crater rim-to-rim diameter and central peak height is summarized in the following table and graph:

Researcher	Applies to crater dia. km	Equation
Wood 1973	> 35km	$H_{cp}=0.006*(D_{rc}^{1.28})$
Hale and Grieve 1982	> 17km - < 51km	$H_{cp}=0.000589*(D_{rc}^{1.969})$

Table 3 - Crater to central peak height relationships

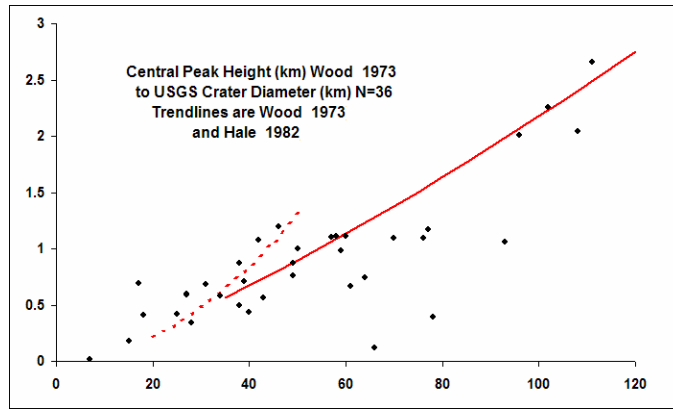


Figure 9 - Diameter to Central Peak Height Relationships after Hale and Grieve 1982 and Wood 1973

As noted above, Wood and Andersson better defined diameter to central peak height relationships for young fresh craters ([Wood and Andersson 1978](#)).

That Pike did not record central peak heights and that Hale and Head did not publish a catalogue of central peak heights creates an amateur research opportunity ([Pike 1976](#), [Hale and Head 1979](#)). Pike identified about 80 craters as having a central peak that are on LTO 100-meter accuracy maps, but for which there is no currently published 100-meter accuracy central peak height measurements. A 100-meter accuracy central peak height measurement might be recovered for these craters from the LTO maps.

2.8 NASA Catalogue of Lunar Nomenclature (NCLN) 1982

After Wood's departure from the Lunar & Planetary Institute in 1973, Wood's work was continued on farside craters by Leif Andersson under the direction of Ewen A. Whitaker. The combined Wood-Arthur and Andersson-Whitaker catalogues were published in 1982 by [Andersson and Whitaker 1982](#). [Andersson and Whitaker 1982](#) is often referred to by its common title - the NASA Catalogue of Lunar Nomenclature (NCLN). The NCLN contained a reduced data set: only crater diameters are reported, not depths. Depths are rounded to whole kilometers.

The [NCLN](#) contains no statement of uncertainty for crater diameters.

The [NCLN](#) also sought to reconcile IAU recognized features with NASA feature assignments. Leif Andersson, who passed away shortly before the publication of the NCLN, was honored post-humously by assignment of his name to C. Andersson, a 13 kilometer diameter crater at S49.7, W95.3. Jonathan McDowell digitized the NCLN in 2004 ([McDowell 2004](#)).

1995 saw the first publication of the GPN by Batson and Russell (Batson and Russell 1995). The current online version of the GPN is accessible over the internet ([USGS 2006b](#)).

3. Measurements based on the Clementine era

3.1. 900-1000 meter accuracy depths - Clementine Digital Elevation Models (DEMs)

1994 saw the Clementine multi-spectral lunar imaging mission. Clementine took multi-spectral images of the lunar surface, took photographic stereograms, and using a laser altimeter and ranging instrument (LIDAR) located absolute elevations for approximately every 512 square kilometers of the lunar surface with spacing varying between 20 and 100 kilometers depending on terrain ([USGS 2002](#)). Clementine collected 72,548 LIDAR elevation points between 79° south and 81° north ([USGS 2002](#)). Clementine LIDAR points have a vertical accuracy of 130 meters ([Archinal *et al* 2005](#)). Figure 10 shows a plot of Clementine LIDAR altimeter points from about 45° north to the north polar limit.

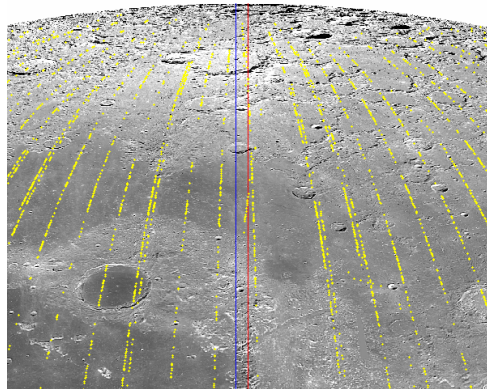


Figure 10 - Clementine LIDAR points. Image – LTVT

LIDAR technology can measure the distance between two points with a high degree of precision and reliability between a known and an unknown point, but the vertical accuracy of Clementine LIDAR points is dependent on the accuracy of the orbital model that provides a reference position of the satellite with respect to the center of the lunar body. The Clementine spacecraft was a moving orbiter of the Moon, a body whose gravitational field varies greatly ([Konopliv *et al.* 1998](#)). Because of variations in the Moon's gravitational fields, the orbits of lunar spacecraft generally are unstable ([Bell 2006](#)).

In 1994, Zuber, Smith and Lemoine *et al* produced the first accurate global topographic model of the Moon using Clementine LIDAR data, named the Goddard Lunar Topography Model-1 (GLTM-1) ([Zuber, Smith and Lemoine *et al* 1994](#)). In 1997, the accuracy of GLTM was improved (GLTM-2) ([Smith *et al.* 1997](#), [Lemoine *et al.* 1997](#)). The GLTM-2 model had a vertical resolution of 100 meters and a horizontal resolution of 2.5°. An improved GLTM-2B data set with a horizontal resolution of 0.25° or 900 meters is available by internet distribution ([NASA and Washington Univ. 2006a](#)). The following figure plots the GLMT-2B topographic model. Light areas are higher in elevation; darks areas are lower. The GLTM-2B model is valid to north/south 78° lunar latitudes.

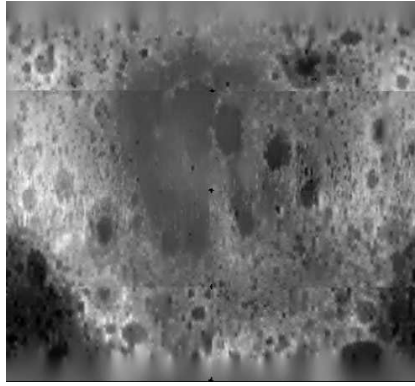


Figure 11 - Plot of GLTM-2B data from [NASA and Washington Univ. 2006a](#). Image - author

These digital elevation models have a low-topographic resolution with respect to individual crater features as compared to earlier stereo-photo-comparator elevation maps, including the 1964 [Topographic Lunar Map](#) or the mid-1970s [Lunar Topographic Orthophotomap \(LTO\) series](#).

Although the LIDAR altimeter points have a much higher level of accuracy at widely-spaced measuring points, once combined with stereograms into a digital elevation model, the accuracy of the final digital elevation model is reduced. The reduction in horizontal resolution of 100-150 meters in Clementine visual band stereograms to 1 kilometer resolution bins in a final lunar digital elevation map also was dictated by the need to conserve computing resources:

Images are matched for every other pixel in the overlap region in each stereo pair - matching every pixel would unfortunately quadruple the expected processing time of four months. . . . The sampling spacing of matched points, every 2x2 pixels, although smaller than a final 1 km DEM pixel size, can provide ~50-100 height measurements per DEM pixel for a single stereo pair since the UVVIS image pixel size is 100-150 m/pixel. The DEM pixel size of 1 km, although lower in resolution than the original UVVIS images, is useful for two purposes: 1) it compensates for most gross navigation errors in camera pointing, and 2) it allows the averaging of many height points contained within each 1x1 km pixel, thus improving the topographic signal to noise ratio over that of a single stereo matched point [[Cook *et al.* 2000](#)].

Using a combination of Clementine LIDAR elevation data and stereograms, Rosiek *et al.* produced a digital elevation map of the north and south lunar poles between 64° north and south latitudes and the north and south lunar poles with a vertical accuracy of approximately 180 meters ([Rosiek et al. 2001](#)). Rosiek *et al.* merged a Clementine LIDAR digital elevation map, Clementine stereophotos, and pre-existing shaded relief maps into an updated full-Moon LIDAR topography map with a 1km horizontal resolution ([Rosiek et al. 2002](#), [USGS 2002](#)). The vertical error of the LIDAR topography map is 180 meters at the north pole and 164 meters at the south pole. This dataset forms one core of the USGS Map-A-Planet online application and its option to plot a “Clementine LIDAR topography” map ([USGS 2006d](#), [USGS 2006e](#)). The 2002 Rosiek *et al.* map also is available in a petal leaf format ([USGS 2002](#)).

Cook *et al.* prepared a whole Moon digital elevation model based on a 5km and a 1km horizontal resolution in order to better reduce noise in vertical measurements. The resulting models had a +-300 meter vertical uncertainty in 5km horizontal model and a +-100 meter vertical uncertainty in the 1km model. ([Cook et al. 2002](#)).

Figure 12 shows a Clementine digital elevation map in Mercator projection of the whole Moon ([Archinal et al 2006c](#)).

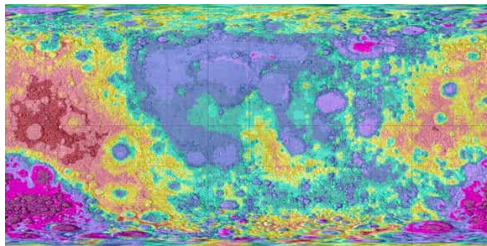


Figure 12 - Full Moon Topography Mercator Projection from [Archinal et al 2006c](#). Image - USGS

The [Rosiek et al. 2002](#) digital elevation map was combined with an air-brush terrain map of the lunar surface with 900 meter per pixel resolution in USGS Map Series 1-2769 ([USGS 2003](#)). The I-2769 datasets form another core of the U.S.G.S. Map-A-Planet online application familiar to many amateur lunar observers. USGS Series 1-2769 is the map that displays as shaded-terrain relief in USGS Map-A-Planet renderings of the lunar surface.

Rosiek continued refinement of the 2002 model, correcting for errors in the 1994 CLCN, and in 2006 issued a revised whole Moon topography model – the ULCN 2005 Topographic Model ([Archinal et al 2006a](#), [Archinal et al 2006b](#)). On 18 January, 2007, the U.S.G.S. internet distributed the ULCN 2005 topographic DEM ([Archinal et al 2006c](#)). The ULCN 2005 DEM can be displayed using USGS using private vendor software licensed by the USGS for free public redistribution ([Archinal et al 2006c](#), [USGS 2006f](#)). The freeware also allows to user to register images to the DEM, to overlay DEM contours onto a user image, and to graph line-of-sight elevation profiles.

The following figure from the ULCN 2005 topographic model shows a DEM and contour plot for the same region surrounding Aristoteles, Eudoxus and Bürg as is depicted from the 1964 [Topographic Lunar Map](#), above at Figure 1. The 200 meter contours in this DEM excerpt are relative to a baseline lunar radius of 1,737.4 kilometers:

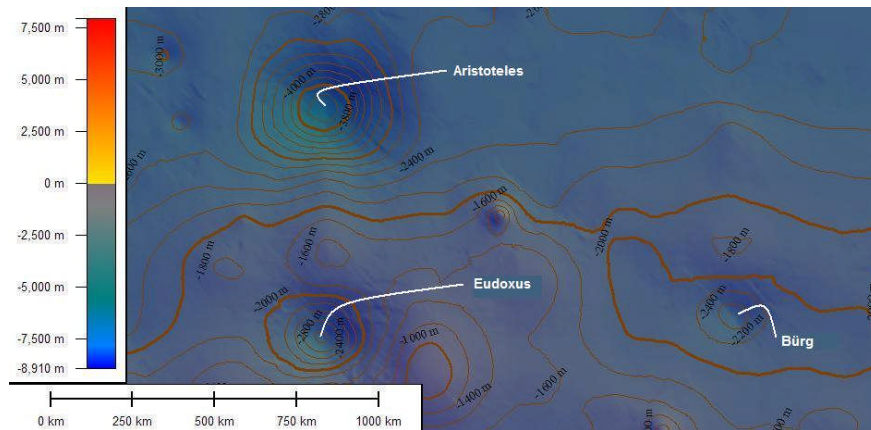


Figure 13 - ULCN 2005 topographic DEM (Excerpt for the region surrounding Aristoteles, Eudoxus and Bürg, image covers approx. 12° lunar latitude by 20° longitude). Image – USGS Dlgv32 Pro

Although of low-resolution compared even to the 1964 TLM, the ULCN 2005 topographic DEM can provide useful information with respect to large craters. The resolution of the DEM is too low to capture a sharp crater rim. The DEM does provide information on the relative height of larger crater floors to surrounding plains as shown in the following figures:

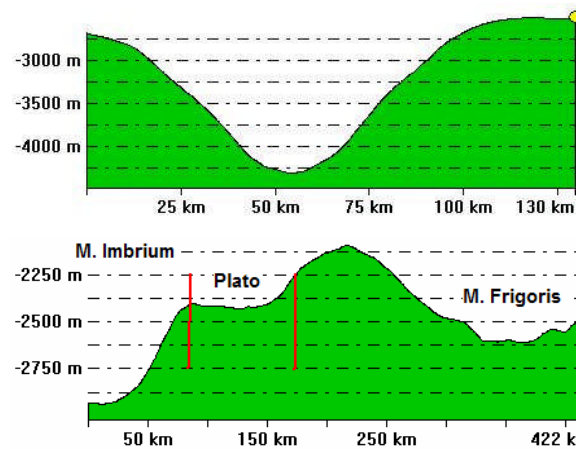


Figure 14 - Profiles of Aristoteles (top) and of Plato (bottom) from M. Imbrium to M. Frigoris at W10 longitude generated from the ULCN 2005 topographic DEM ([Archinal et al 2006c](#)). Image – USGS Dlgv32 Pro

See Figure 13 with respect to the profile sight-line for Aristoteles and Rühl Charts 3, 4 and 11 for Plato profile sight-line.

In 2007, Rosiek *et al* announced the computation of preliminary revised 1 kilometer and 5 kilometer resolution DEMs based on the new ULCN 2005 model ([Rosiek *et al* 2007](#)). The revision updates Rosiek *et al*'s 2002 DEM and covers 35% of the Moon's surface. 66% of the DEM tiles have a vertical accuracy between 300 and 500 meters; 33% have a vertical accuracy between 500 and 1000 meters.

3.2 137-219 meter accuracy depths – Clementine Control Point Networks

Interplanetary body control point networks, like their terrestrial counterpart, provide for the location of local features on a body's surface where the body's fundamental points are obscured by the local horizon ([Schirmerman, U.S. Defense Mapping Agency 1973](#) at Sec. 3.0). The local control points provide an intermediary reference between the feature's position and fundamental points. In addition for computing feature positions, control networks can be used register lunar images to maps of the Moon's surface. For the Moon, fundamental points are usually taken as the center of the Moon's spheroid and/or the center of the floor of satellite feature Möstling A at S3.2, W5.2 lunar latitude and longitude.

In 1994 and prefatory to analysis of Clementine mission images, Davies *et al.* prepared an updated control point network of 1478 points, 1286 of which are on the nearside, commonly known as the Unified Lunar Control Network (ULCN 1994) ([Davies *et al.* 1994a](#), [USGS 2006c](#)). ULCN 1994 is based on improved processing of data from the Apollo 15 control system, on imagery from the Mariner 10 and Galileo missions, and on Earth-based photography ([USGS 2006c](#)). ULCN points have a horizontal accuracy of 100 meters to 3km and vertical accuracy of a few kilometers ([Archinal *et al.* 2005](#), [USGS 2006c](#)). ULCN 1994 control points are generally located on the floors of satellite feature craters. ULCN 1994 is included as a data file in Mosher's and Bondo's Lunar Terminator Visualization Tool, discussed below, or is available by internet download from the USGS ([Mosher and Bondo 2006](#), [Davies *et al.* 1994b](#)).

In 1997 as part of processing Clementine images into mosaics, Merton Davies and Tim Colvin created the Clementine Lunar Control Network (CLCN) – a set of 271,634 control points ([USGS 2006c](#)). The CLCN was used to register over 40,000 Clementine images into the digital elevation models discussed above. The accuracy of the CLCN was called into question and in August 2006, Archinal *et al.* issued a corrected set of 272,931 3-D coordinates – the Unified Lunar Control Network 2005 (ULCN 2005) ([Archinal *et al.* 2006b](#)).

The ULCN 2005 has a mean vertical uncertainty of 137 meters, with a first standard deviation error of 219 meters ([Archinal *et al.* 2006c](#) at 2). The mean horizontal position accuracy is 335 meters with a maximum three standard deviation error of 5.1 kilometers ([Archinal *et al.* 2006c](#) at 3). The control points have a density of one point per 46 km², or one point every 6.8 kilometers.

In 2007, Archinal *et al* announced the completion of the ULCN 2005 Control Network and Lunar Topographic Model ([Archinal et al 2007](#)). Planned improvements to the control network and model have been placed on hold due to United States federal budget cuts.

3.3. 100-325 meter accuracy crater diameters - Clementine base map images

Clementine visual images were taken at too high a sun angle in order to be useful for shadow depth or height measurements ([Lena 2006](#)). But Clementine 750nm base map images can be used for the study of horizontal crater diameters.

The Clementine 750nm base map images, also available from USGS Map-A-Planet, have a horizontal resolution between 100 to 325 meters and typically cover about 40 square kilometers ([USGS 2006e](#)). The USGS Map-A-Planet Clementine images display in a rectified format and can be used to measure crater diameters with common desktop paint utilities. The USGS Map-A-Planet applet displays the resolution of the image at the bottom of screen in pixels per kilometer.

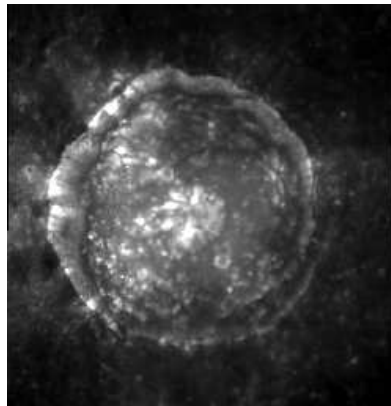


Figure 15 - C. Plinius (dia. 41.2 km) at 237 meters per pixel resolution. Image - USGS Map-A-Planet

Clementine base map images are also available from NASA Planetary Data Services as collections CL-3001 through CL-3015 ([NASA 2006a](#)).

3.4 20-100 meter accuracy crater diameters - Clementine HiRes polarimagemap

Two other Clementine image series are available at higher resolutions, but finding and using the images related to specific features requires more effort. The images in these collections do not display in a rectified format, making reduction of crater diameters from the images complicated.

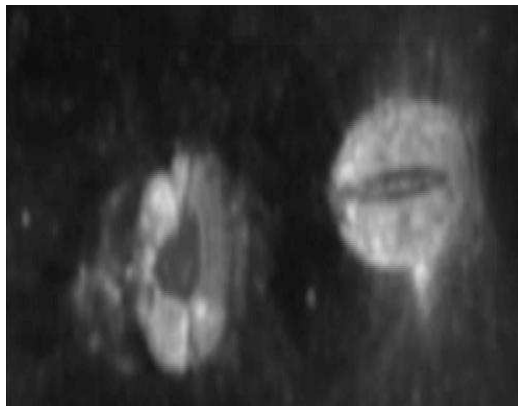


Figure 16 – Messier A (dia. 13.25 km) and Messier (dia. 11.63 km) from CL-4013, Image UI03S045, at 100 meters per pixel. Image - NASA PDS

The PDS Clementine CL-4001 through CL-4078 image series provides a slightly higher precision of 100 meter horizontal resolution over the CL-3000 series ([NASA 2006b](#)). The PDS Clementine Data Node also provides internet distribution of the Clementine HiRes polar image map with a 20-30 meter horizontal resolution as collections CL-6001 through CL-6022 ([NASA 2006c](#)). These images are not rectified.

Clementine 750nm base map, HiRes and HiRes polar images are stored at the NASA Washington Univ. (St. Louis) Planetary Data Systems (PDS) Clementine Data Node ([NASA-Washington Univ. 2006b](#)). The PDS Clementine Data Node provides a browser image viewing interface for some collections. NASA-JPL also provides a desktop viewer compatible with Clementine PDS stored images for either Windows, Apple/Macintosh or UNIX operating systems ([NASA and JPL 2006](#)).

3.5. Digital elevation models from Clementine data vs. Apollo era stereophotograph measurements

Because Clementine digital elevation models aggregate vertical elevation data in 1,000 meter horizontal bins, they do not provide a significantly improved level of vertical accuracy (180 meters by [Rosiek *et al.* 2001](#) and 100 meters by [Cook *et al.* 2002](#)) as compared to the 61 horizontal meter by 20 vertical meter accuracy achieved by the Apollo era [Lunar Topophotomap series](#) or the 160-500 horizontal meter and 30-115 vertical meter accuracy of the Apollo [Lunar Topographic Orthophotomap series](#).

Digital elevation models on a 1,000 meter horizontal resolution also have limitations with respect to small craters depths for features located on irregular terrain. At a 1km resolution, the odds of having elevation points on a rim crest or crater floor become small. Conversely, with respect to larger craters, digital elevation models make craters more amenable to volumetric fitting, similar to that explored by Hale and Grieve in the 1980s based on digitization of the LTO map series ([Hale and Grieve 1982](#)).

In this respect, Clementine era digital elevation models have a lower vertical resolution than the Apollo era data discussed above. Conversely, the Clementine digital elevation models have coverage over the entire Moon with all measurements being expressed with respect to a 1737.4 kilometer idealized surface.

Control point systems like ULCN 1994 and ULCN 2005 have a vertical uncertainty greater than the Apollo era data discussed here.

4. Measurements from the Earth-based radar interferometry era (1997-2006) - 20 meter vertical accuracy and 150 meter horizontal accuracy

Earth-based radar mapping of the Moon began in the post-World War II era using surplus military antennae. Thompson produced a whole nearside Doppler radar map of the Moon to a resolution of 1 kilometer using the Haystack and Arecibo radio observatories ([Thompson 1979](#)).

Stacey continued and expanded this work using the Arecibo observatory by developing new Doppler radar analysis techniques that could image to a 20 meter resolution ([Stacy et al. 1997](#)).

Since the mid-1990s, four researchers – B.A. Campbell, D.B. Campbell, N.J.S. Stacy and J.L. Margot - have pioneered the use of radar interferometry to prepare high resolution maps of lunar craters ([Stacy et al. 1997](#), [Margot et al. 2000](#) and [Campbell et al. 2004](#)). Their efforts have been principally focused on mapping possible ice deposits at the lunar poles ([Stacy et al. 1997](#), [Margot et al. 2000](#) and [Campbell et al. 2006](#)). In the search for lunar ice deposits, Margot and B.A. Campbell each illustrate how the technique is usually used to achieve 400 meter resolution near the lunar limb, but can be pushed to a 150 meter horizontal and a 20 meter vertical resolution ([Margot et al. 2000](#) and [B.A. Campbell et al. 2005](#)).

Margot *et al.* prepared a detailed topographic map of the crater Tycho with a horizontal resolution of 200 meters and a vertical resolution of 20 meters using Earth-based radar interferometry ([Margot et al. 1999a](#)). Margot *et al.* found that Tycho's central peak rises 2,400 meters above the mean crater floor and that the crater's depth was 4,700 m between mean rim and mean floor. Compare with Apollo era estimates in Table 1. A radar map image of Tycho can be found in Figures 5 and 6 of [Margot et al. 2000](#).

Margot *et al.* also prepared the north and south lunar pole radar interferometer maps of the north and south lunar poles above north-south latitudes 87.5° to a horizontal resolution of 150 meters and a vertical resolution of 50 meters ([Margot et al. 1999b](#)).

B.A. Campbell *et al.* produced a 300 meter horizontal resolution radar map of Posidonius ([Campbell et al. 2003](#)). A 400 meter horizontal resolution radar maps of the lunar south pole and for the lunar nearside have been produced ([Campbell et al. 2004](#), [Campbell et al. 2005](#)).

B.A. Campbell *et al.* prepared a 20-meter horizontal resolution image of the Cobra's Head on the Aristarchus Plateau and a digital elevation model of Reiner Gamma formation ([Campbell, Carter and Campbell *et al* 2006](#)).

D.B. Campbell *et al.* achieved 20 meter vertical resolution in mapping C. Shoemaker at the lunar south pole ([Campbell and Carter 2006](#)). In October, 2006, based in part on this increased resolution, D.B. Campbell *et al.* concluded that it was unlikely that there were ice deposits at the south lunar pole ([Campbell *et al.* 2006](#)).

Like shadow measurements, the accuracy of Doppler radar is not uniform across the nearside. Shadow measurements decrease in accuracy closer to the lunar limb. Doppler radar is more accurate (300-400 horizontal meters) closer to the lunar limbs but decreases to 900 meters for features near the central annulus of constant radar signal return. ([Margot *et al.* 2000](#), [Campbell *et al.* 2005](#)).

Although Doppler radar studies are currently focused on lunar ice at the poles, the north and south lunar pole digital elevation models with 20 meter vertical resolution could be used to prepare enhanced accuracy crater depth, diameter and volume catalogues. As of this date they have not be used for that purpose. Using Earth-based Doppler radar, a 20 meter vertical resolution digital elevation map of the entire nearside appears technologically feasible.

5. Local feature DEMs from Shape-from-Shading (SFS) photoclinometry

As shown in Figure 14 above, whole-Moon DEMs based on orbiter stereophotography and LIDAR measurements have low detail resolution even for large craters. An alternative

method for rendering localized DEMs is photoclinometry based on “shape from shading” (SFS).

The basic concept underlying SFS photoclinometry is that a lunar surface reflects light in proportion to Sun’s altitude in the lunar horizon system of the feature to be studied.

Deleted:

5.1. Computationally complex SFS algorithms after Hapke and Kirk

If a surface is a uniform diffuse-light-scattering surface – it is a Lambertian surface.

Few lunar surfaces reflect light in a uniform manner due to variations in surface composition.

Hapke provides a computationally complex method for quantifying the reflectance of lunar surfaces (Hapke 1993). Hapke’s methods are incorporated by Kirk into a software package called *Integrated Software for Imagers and Spectrometers (ISIS)* (USGS 2007, Kirk, Barrett and Soderblom 2003). ISIS currently is used by researchers on Mars orbiter missions to convert Mars images to DEMs. ISIS will be used on future lunar missions, described below, for the same purpose.

5.2. Reduced computational SFS algorithms after Wöhler, Hafezi and Lena *et al*

Wöhler and Hafezi and Lena, Pau and Phillips *et al* described a computationally reduced algorithm for constructing local feature DEMs that measures lunar feature elevations to accuracy similar to more intensive Kirk-Hapke SFS algorithms. (Wöhler and Hafezi 2005, Lena, Pau and Phillips *et al* 2006). A reduced level of computation is achieved, in part, by assuming that the lunar surface to be measured is a uniform diffuse-light-scattering Lambertian surface (Wöhler and Hafezi 2005).

Deleted: an

Deleted: more detailed

Deleted: from a variant of photoclinometry termed “shape from shading” (SFS)

Deleted: The core assumption of the SFS-photoclinometry technique is that

Deleted: surface. A lunar surface that meets this uniformity criteria – also called a

Deleted: surface - reflects low-angle light in portion to the height of the

Many classes of lunar features do not meet this basic criteria and are excluded as suitable candidates for SFS-photoclinometry. Such classes of features have albedo variations related to the changes in surface mineral composition. Examples include radial banded craters like Bessarion, dark mantle pyroclastic deposits near Rima Bode, the cryptomare in Schickard, magnetic swirls like Reiner Gamma, dark halo craters like Copernicus H, dark-rayed craters like Dionysius, and, in high-altitude lighting, bright-rayed craters like Tycho. Not all bright-rayed craters are excluded. As discussed below, some bright-rayed craters reflect uniform-diffuse light in the visible band under low-angle solar illumination.

SFS-photoclinometry works best in low Sun illumination – less than 20-30°. Low illumination angles imply the SFS works best on features with a height above surrounding plain of one kilometer or less. Under low illumination, terrain on the shadow side of a feature still will reflect light. Information on terrain gradient from reflectance will not be lost in dark-deep shadows, as occurs for tall mountains and ridge systems on the edge of basins.

Where a lunar feature does meet the basic criteria of uniform diffuse reflection, the SFS-photoclinometry algorithm described by Wöhler and Hafezi and Lena, Pau and Phillips *et al* can be applied. The Wöhler and Hafezi algorithm structurally is forward-fitting (Kirk, Barrett and Soderblom 2003 at 3-4). Conceptually, the SFS algorithm is simple:

A computational DEM matrix is initialized with zero elevation heights;

A seed albedo of a flat or nearly flat surface within the user's image is found based slope analysis determined from classical shadow measurements;

The height and albedo of each pixel in the DEM matrix is estimated from pixel's current estimated slope;

The residual error between each pixel's computed albedo in the computational DEM matrix and the user's image is estimated;

The height of each pixel in the DEM matrix is updated based on the pixel's residual error; and, The DEM matrix is recomputed until the residual error of each pixel is minimized ([Lena Pau and Phillips *et al* 2006](#), [Wöhler and Hafezi 2005](#)).

The Geologic Lunar Research Group (GLR Group) has applied this SFS method to a variety of lunar features, discussed below.

5.2.1.20%+ height accuracy – SFS-photoclinometry of craters and miscellaneous features using the Wöhler and Hafezi algorithm

Formatted: Heading 3

Examples of Lambertian surfaces on the Moon that can meet the basic photoclinometry criteria of uniform diffuse surface reflectance include wrinkle ridges on mares, straight faults on mares and some craters.

Wöhler and Hafezi demonstrated SFS-photoclinometry on these classes of features ([Wöhler and Hafezi 2005](#)). Examples of their local feature DEMs for a wrinkle ridge, straight fault and part of a large crater are shown in Figure 17 to Figure 19.

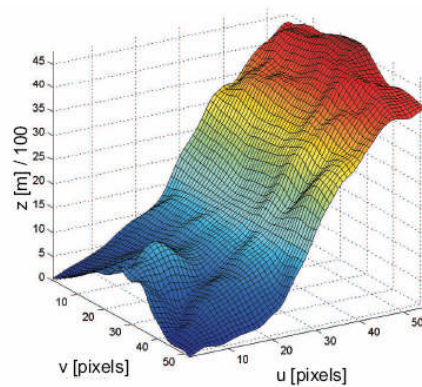


Figure 17 – Local feature DEM for part of the East slope of Copernicus (radius ~ 46.5 km). Image - [Wöhler and Hafezi 2005](#)

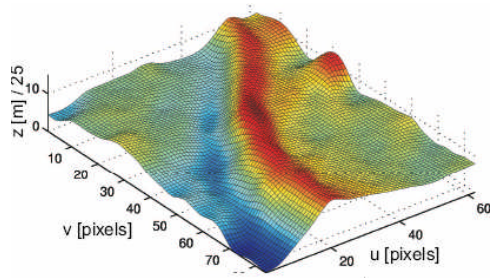


Figure 18 - Local feature DEM for a mare wrinkle ridge south-west of crater Aristarchus.
Image - [Wöhler and Hafezi 2005](#)

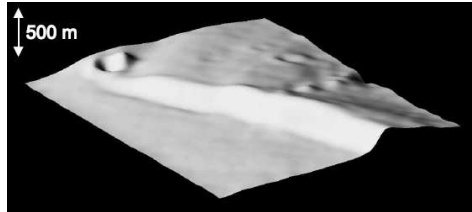


Figure 19 - Local feature DEM for the north end of Rupes Bürg. (~ 10 km by 10 km)
Image - [Wöhler and Hafezi 2005](#)

Resolution in these local feature DEMs is much greater than whole-Moon DEM resolution shown in Figure 13 above. The modern depth estimate for Copernicus is 3,800 meters ([Pike 1976](#)).

Per GLR Group members Wöhler, Lena and Lazzarotti, the typical standard error for height measurements obtained through SFS-photoclinometry is 20% ([Wöhler, Lena and Lazzarotti et al 2006](#)). Lighting anomalies can produce height artifacts, *e.g.* – the crater in the upper left-hand corner of Figure 19 ([Wöhler and Hafezi 2005](#)).

Deleted: Geologic Lunar Research Group (
Deleted:)
Deleted: t

Because many wrinkle ridges, straight faults and craters may have albedo variations confounded by changing surface mineral composition, SFS-photoclinometry should be applied to such features with caution. Application of multiple measuring techniques to a feature (shadow measurements and light profiles) and false color ratio imagery can minimize spurious measurements of heights and corroborate the photoclinometry result (e.g. [Lena, Wöhler and Bregante et al 2006](#), [Wöhler and Hafezi 2005](#)).

5.2.2. **10%+ height accuracy, less than 100 meters – SFS-photoclinometry of lunar domes using the Wöhler and Hafezi algorithm**

Formatted: Heading 3

Deleted: Less

Domes are one of the best lunar features that meet the basic SFS-photoclinometry criteria of uniform diffuse reflectance. That lunar domes reflect diffuse light uniformly is known to many amateurs who have conducted a futile search for these features in high-altitude lighted Clementine images. Lunar domes generally are indistinguishable from their surroundings in Clementine 750nm base map images precisely because they reflect light uniformly and at the same intensity as the surface materials that surround an individual dome. This characteristic of high-altitude Clementine photographs of lunar domes makes those images unsuitable for stereophotography, but conversely shows that lunar domes are good candidates for SFS-photoclinometry ([Wöhler, Lena and Lazzarotti et al 2006](#)).

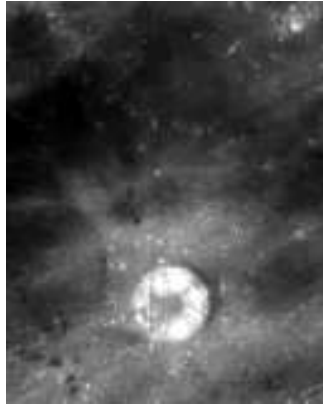


Figure 20 – Six lunar domes north of C. Hortensius, ~ 6 to 12 km in dia, contained within the boundaries of this Clementine 750nm base map image are almost invisible. Hortensius' dia. is 14 km. Image - USGS Map-A-Planet

GLR Group members Kapral and Garfinkle published a catalogue of approximately 2,500 verified and unverified domes and other miscellaneous features ([Kapral and Garfinkle 2005](#)). The Kapral-Garfinkle catalogue is a compilation of domes compiled from approximately 25 journal and other sources, including the Journal of the Assoc. of Lunar and Planetary Observers. Of those entries, approximately 750 involve verified and unverified domes (as opposed to miscellaneous features) and 186 verified and unverified domes have associated height measurements. The distribution of those 186 domes is plotted in Figure 21. The distribution of 751 verified and unverified domes with known diameters do not differ significantly from Figure 21 and are not plotted separately here. A digitized catalogue is provided by the GLR Group ([Kapral and Garfinkle 2005](#)). This catalogue is also plotted by the GLR Group on a copy of the LAC charts ([Shaw 2006](#)).

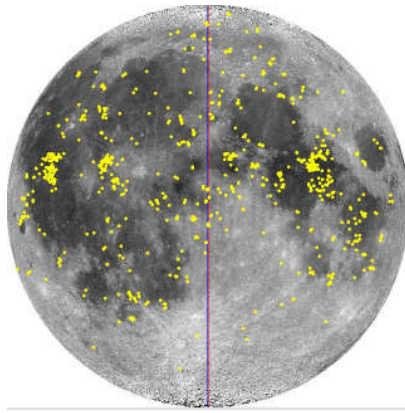


Figure 21 - Distribution of 186 verified and unverified domes with listed heights per [Kapral and Garfinkle 2005](#). Image - LTVT

The morphology of domes also is favorable to application of SFS photoclino-

metry. Lunar domes tend to be about one kilometer in height and at most 20 kilometers in diameter

(Hiesinger and Head 2006 at 42). At low solar illumination, lunar domes do not cast dark, deep

shadows on the shadow-side of a feature. The distribution of heights of verified lunar domes

from Kapral and Garfinkle are shown in Figure 22. Ninety-five percent of the domes have

heights less than 1.2 kilometer; sixty-six percent have heights less than 400 meters.

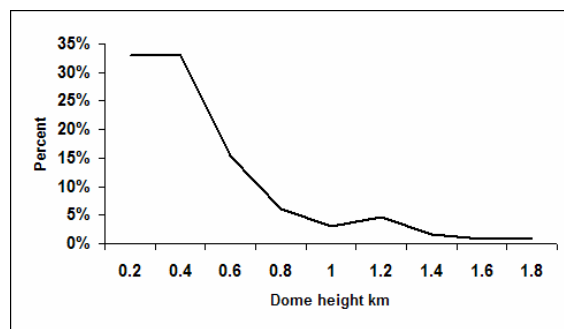


Figure 22 - Distribution of heights of 130 verified domes per Kapral and Garfinkle 2005.

The GLR Group's Wöhler *et al* described a SFS-photoclinometry technique that uses dome albedo to measure the height of lunar domes down to below a 100 meter level of precision (Wöhler, Lena and Lazzarotti *et al* 2006). The stated precision is 10 percent for dome heights and 5 percent for dome diameters (Wöhler, Lena and Lazzarotti *et al* 2006). Traditional shadow measurements of lunar dome heights yield "slope and height values consistent with those obtained by the [SFS] image-based 3D reconstruction . . . [Id]."

The GLR Group has completed many topographic DEM studies of individual domes using SFS-photoclinometry. A partial representative list of studies concern unlisted domes analysis and re-evaluation of known dome fields (Lena, Wöhler and Bregante *et al* 2007 (unlisted dome near Messier), Wöhler, Lena and Lazzarotti *et al* 2006 (Cauchy and Hortensius domes fields), Lena, Pau and Phillips *et al* 2006 (unlisted dome near the Valentine dome), Lena, Wöhler and Bregante *et al* 2006 (unlisted dome on the floor of the Petavius)).

Deleted: Evans illustrates a version of the photoclinometry technique using a simple Excel spreadsheet to measure lunar dome heights (Evans 2006). ¶

5.3. 20%+ height accuracy – SFS-photoclinometry of lunar domes using the minimal SFS algorithms of Carlotto 1996

Evans, an amateur GLR Group member, described a SFS-photoclinometry technique, using simple Excel spreadsheets, to measure lunar dome heights after the computationally minimal technique of Carlotto (Evans 2006a, Carlotto 1996). Evans' Excel spreadsheet can be obtained through the *Selenology Today* website (Evans 2006b).

In Carlotto's method, SFS computation is reduced to a minimum by using astrophotography software to rotate a lunar dome so the apparent solar azimuth incidence is 270°. Evans demonstrated that Carlotto's method produces elevation models that have an accuracy of about 9% of the elevations obtained in the GLR Group lunar dome studies (10%) discussed above. This implies about a 20% height accuracy for lunar domes.

In addition to the basic SFS criteria of uniform reflectance, Carlotto notes that his method is limited to scenes illuminated by Sun altitudes of less than 20-30°. Evans recommends that the method only be used for features between 30° N/S lunar latitude due to the effect of foreshortening. The end-result of this SFS process are pixel scaled elevation maps similar to Figure 18, above, or a wireframe model similar to Evans' rendering of the 12.2 kilometer diameter Cauchy Omega dome.

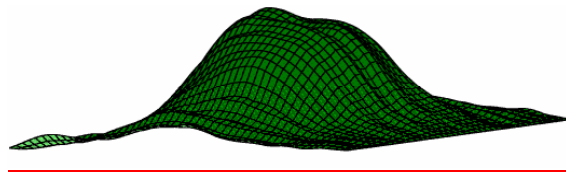


Figure 23 – A DEM wireframe rendering of Cauchy Omega. Image – Author from Evans 2006b data.

6. Modern amateur Earth-based astrophotography, shadow measurements and DEMs

How accurate can amateurs measure crater depths and feature heights from the Earth using modern tools? Has amateur astrophotography progressed to the point in the last three years, where reasonably accurate height and depth shadow measurements from lunar photographs? Is their accuracy sufficient to compete with traditional Earth based micrometer measuring? Can they provide useful topographical data for specific features that supplements digital elevation models prepared from lunar orbiters?

The major components of error in making feature height or depth measurements by the classical shadow method include:

- Accurate ephemeris;
- Accuracy in determining feature coordinates;
- Topographic slope variations;
- Atmospheric seeing;
- Computational error; and,
- Technique in measuring shadow length ([Davis 1997](#)).

6.1. 10% height – Traditional amateurs shadow measurements with microfilament meters

Amateur Bill Davis describes how he tested the accuracy of his use of a microfilament to measure the height of features on the Moon (Davis 1998). Davis called the ALPO's Dr. John Westfall. In the context of that work, Westfall suggested using the Lunar Topographic Orthophotomaps as a practice baseline. From 119 micrometer measurements, Davis found he estimated heights to within a 10% accuracy of the LTO map value for Mt. Harbinger and 18 other lunar mountains. Davis commented that the best measurements were made with a solar angle between 3 and 6 degrees.

Davis simulated shadow measurements for a 1,500 meter central peak and found that a 1 degree negative slope of a surrounding mare results in about a 23% over estimation of height; a 1 degree positive slope results in about a 16% under estimation of height ([Davis 1997](#)). With respect to positive relief dome heights, Lena, Pau and Phillips *et al* suggest compensating for this confounding factor by estimating feature height from the difference between a morning and evening elevation measurement ([Lena, Pau and Phillips et al 2006](#)).

6.2 Lucky Imaging astrophotography combined with shadow measuring and light curve profiles

Recently, advanced amateurs like Paolo Lazzarotti regularly make lunar images with linear resolutions down to 0.11-0.22 arcsecs per pixel that correspond to sub-kilometer linear distances (see [Wöhler et al 2007](#) at p. 76). For a lunar feature at N0, E0 when the Moon is at 384,440 kilometers distance, 0.11 arcsecs corresponds to about 200 meters.

There are competing parameters that affect the resolution of shadows in modern astrophotographs – the moving terminator versus repeated imaging over time.

The shadow cast by a lunar feature moves. At low oblique sun angles, the shadow cast by feature will be longer than 200 meters even though the feature is less than 200 meters in height or depth. But at the equator, the terminator moves across the lunar disk at about 510 meters a minute. At 45 degrees north latitude, it moves at about 360 meters a minute.

Modern high-resolution amateur astrophotographs usually are acquired over time using the technique of “Lucky imaging” ([Law, MacKay and Baldwin 2006](#), [Tubbs 2004](#)). The astrophotographer (1) takes many images over several minutes, (2) selects images with the best point-spread function during a moment of atmospheric calm within a larger interval of atmospheric turbulence, (3) registers the image by cross-correlation, (4) averages the correlated images, and (5) applies filtering techniques such as convolution to the averaged image. The characterization of the technique as “lucky imaging” comes from the probability associated with taking an image during a moment of atmospheric quiet within a given interval of general atmospheric turbulence. During the first step of the lucky imaging process, the feature shadow moves between taking of individual images. Averaging images results in a fuzzy position of the shadow during the imaging session.

Jim Mosher and Henrik Bondo implemented a modern graphical user interface for the manipulation of and feature plotting on user lunar photographs – the Lunar Terminator Visualization Tool (LTVT) ([Mosher and Bondo 2006](#)). LTVT includes a shadow measuring tool. In order to model the accurate position of the lunar terminator and to determine the lunar azimuth and altitude of the Sun at a lunar coordinate, LTVT downloads high accuracy Jet Propulsion Laboratory (JPL) lunar ephemeris files. To assist in the accurate determination of lunar coordinates, LTVT includes a feature for registering a user lunar image to either 1994 or 2005 ULCN points. The shadow measuring tool does not follow the classical mathematical algorithm of MacDonald.

The accuracy of measurements made using LTVT's measuring tool has not been fully tested. LTVT is still in the post-beta revision, development and refinement stage. Initial anecdotal testing indicates that a crater depth accuracy between 5-10% compared to LTO map depths can be achieved with careful technique, including checking image alignment to 1994 ULCN control points ([Wood 2006](#), Mosher, personal communication).

Another useful feature of LTVT, unrelated to shadow measurements but also worth noting, is its ability to easily rectify user lunar images.

Wöhler *et al.* described a topographic study of Rupes Bûrg that applies shadow measuring to advanced modern lunar astrophotographs ([Wöhler et al. 2007](#)). Wöhler *et al.* estimated the height of Rupes Bûrg at approximately 400 meters. Wöhler *et al.* also demonstrated how light profile curve tools, a feature of many common astrophotography software packages, can be used to characterize the topographic profile of lunar ridges. There is no uncertainty statement for height measurements in Wöhler et al. 2007.

The application of traditional shadow measuring techniques to modern "Lucky imaging" high-resolution amateur lunar photographs could benefit from further characterization of the method's accuracy.

Davis's technique of using test measurements based on features on LTO and LTP maps in order to establish an accuracy baseline suggests a method by which amateurs can quantify the reliability of any technique that they use.▼

Deleted:

7. The Future – Geologic DEMs, SMART-1, SELENE and LRO

Calibrating multispectral imaging from the Clementine and Lunar Prospector missions with the spectrographic response of Apollo and Luna mission soil return samples has expanded and changed our understanding of global lunar surface geology (Hiesinger and Head 2006 at 8, 64-65).

The next logical step in the evolution of topographic DEM information and new geologic insights from multispectral remote sensing is the combination of the two data sets into a new geologic atlas of the Moon – updating the thirty-year old Apollo era atlas mentioned above ([USGS, NASA and US Airforce ACIC 197](#)). In 2006, the USGS announced the first results of a pilot project funded by NASA to prepare a new geologic lunar map series on a 1:2,500,000 scale based on updated Clementine multispectral image analysis ([Gaddis et al 2006](#)). Gaddis *et al* includes a preliminary draft of the first quadrangle map produced by the pilot project for the Copernicus area.

New SMART-1 imaging has not been released for public access, as of this paper. Koschny *et al* discussed the distribution of SMART-1 images on the lunar globe ([Koschny et al 2007](#)).

Rosiek *et al.* have experimented using overlapping Lunar Orbiter, Apollo 15 and Clementine images of the Apollo 15 Mt. Hadley landing site to automatically generate digital elevation maps with the precision equal to the TPM series ([Rosiek et al. 2006](#)).

With respect to the SELENE mission to be launched in the summer of 2007, Honda *et al* described initial tests of stereographic mapping software designed to convert stereophotographs into digital topographic models ([Honda *et al* 2007](#)). SELENE's terrain mapping camera has a horizontal resolution of 10 meters/pixel. Software tests on simulated lunar surfaces were able to build DEMs with a vertical accuracy 5 to 25 meters for one standard error. Software tests on an Apollo 15 stereophotograph created a DEM that could resolve craters more than 100 meters in diameter and a rille about 1 kilometer in width. Yokota *et al* also demonstrated SELENE kilometer scale DEM software for the production of orthotopographic terrain maps, again using Apollo era stereophotographs as test data ([Yokota *et al* 2007](#)).

A SELENE mission goal is to prepare a new high accuracy global DEM based on low-altitude orbit stereophotographs. The mission intends to fill-in 80% of the lunar surface not covered by the Apollo era stereophoto LTO maps ([Honda *et al* 2007](#)).

The Lunar Reconnaissance Orbiter (LRO) is scheduled to fly in October 2008. Chin *et al* describes the LRO's topographic-mapping related instruments, including a laser altimeter, an imaging camera and side-looking synthetic aperture radar. Data from these instruments will support new global topographic mapping and detailed mapping of cold traps at the lunar poles with between 15 to 100 meter horizontal resolution ([Chin *et al* 2007](#)).

8. Conclusion

This retrospective on the gathering of higher accuracy lunar crater and feature depth, height and diameter measurements represents one of many of the high-points of the Apollo era explorations. It represented a great-leap forward in our understanding of lunar topography. That effort continued through the Clementine era and subsequent Earth-based radar interferometry and will continue in future orbiter imaging missions.

There is a cautionary lesson-learned in this history. Some measurements from the Apollo era have been lost where catalogues were not preserved by publishing for later historical use.

Hopefully, the future will chart a path towards preserving raw measurements and preventing the loss of hard won lunar data while continuing the USGS-NASA practice of open internet distribution. At the 57th Annual International Astronautical Congress, NASA Chief Administrator Griffin asked that "lunar science data should be openly shared among the science community, just as we do with other planetary science data [[Griffin 2006](#), p. 11]." Griffin suggested the collective sharing and standardized formatting of all data from upcoming lunar missions ([Ellison 2006](#)). In 2006, NASA announced a partnering initiative with the online search engine Google.com to distribute 3-D lunar surface renderings ([NASA 2006d](#)).

For amateurs concerned that pursuit of lunar topographic studies with amateur tools has been deprecated by digital elevation maps generated from orbiter missions, modern lunar astrophotography appears to have a level of precision sufficient to justify follow-up topographic study of individual terrain features. The foregoing review provides an overview of professional studies and resources, so the amateur can avoid duplicative effort, or use existing professional data as a baseline against which to practice technique and/or corroborate their depth-height measurements.

The Appendix describes the method by which a table of higher accuracy crater depth and central peak heights measurements from the Apollo era was developed and matched with the USGS GPN.

The table of digitized Apollo era crater depths is distributed electronically as supplemental material in the following formats:

Pdf -

<http://members.csolutions.net/fisherka/astronote/plan/craterdepth/trans/CraterDepthFeatureName.pdf>

Html -

<http://members.csolutions.net/fisherka/astronote/plan/craterdepth/trans/CraterDepthFeatureName.html>

Csv -

<http://members.csolutions.net/fisherka/astronote/plan/craterdepth/trans/CraterDepthsFeatureName.csv>

LTVT compatible feature plotting files used to generate Figure 3 and Figure 6 can be found at the author's website:

<http://members.csolutions.net/fisherka/astronote/plan/craterdepth/CraterDepthsApolloEra.html#LTVTdatafiles>

The Appendix in Westfall's *Atlas of the Lunar Terminator* remains the best general amateur source for the depths of larger named crater depths (Westfall 2000).

References

Andersson, L.E. and Whitaker, E.A. 1982. *NASA Catalogue of Lunar Nomenclature (NCLN)*. NASA Reference Publication 1097. ([Link](#))

Archinal, B. A., Rosiek, M. R., Kirk, R. L. and Redding, B. L. 2005. Unified Lunar Topographic Model. *Space Resources Roundtable VII: LEAG Conference on Lunar Exploration*, Abstract No. 2060. ([Link](#))

Archinal, B.A., Rosiek, M.R., Kirk, R.L. and Redding, B.L. 2006a. Completion of the Unified Lunar Control Network 2005 and Topographic Model. *37th Annual Lunar and Planetary Science Conference, 2006*. Abstract No. 2310. ([NASA/ADS](#))

Archinal, B. A., Rosiek, M. R., Kirk, R. L. and Redding, B. L. 2006b. A Clementine Derived Control Network and Topographic Model - The Unified Lunar Control Network 2005. *Progress in Planetary Exploration Missions, 26th meeting of the IAU, Joint Discussion 10, 21-22 August 2006, Prague, Czech Republic*. JD10, #26 (Abstract). ([NASA/ADS](#))

Archinal, B.A., Rosiek, M.R., Kirk, L.K., and Redding, B.L. 2006c. The Unified Lunar Control Network 2005. U.S. Geological Survey Open-File Report 2006-1367 (Ver. 1.0). URL: <http://pubs.usgs.gov/of/2006/1367/>, (last date accessed 3 Feb. 2007) (See data file ULCN2005_LPOLY.zip for model)

Archinal, B. A., Rosiek, M. R., Kirk, R. L. , Hare, T. L. and Redding, B. L. 2007. Final Completion of the Unified Lunar Control Network 2005 and Lunar Topographic Model. *38th Annual Lunar and Planetary Science Conference, March 12-16, 2007, League City, Texas*, Abstract No. 1904. URL: <http://www.lpi.usra.edu/meetings/lpsc2007/pdf/1904.pdf> (last date accessed 7 Feb. 2007)

Army Map Service, Corps of Engineers. 1964 (2d). Topographic Lunar Map (West-half and East-half maps). URL: <http://www.lpi.usra.edu/resources/mapcatalog/LTM/>, (last date accessed:

3 Feb. 2007).

Deleted: 2/

Deleted: /

Deleted:).

Arthur, D. W. G. 1974. Lunar crater depths from Orbiter IV long-focus photographs. *Icarus*. 23:116-133. ([NASA/ADS](#))

Batson, Raymond M. & Russell, Joel F. 1995. *Gazetteer of Planetary Nomenclature*. U.S. Geological Survey Bulletin 2129. Washington: U.S. Government Printing Office.

Bell, T. 2006. Bizarre Lunar Orbits. (NASA Press Release). URL:

http://science.nasa.gov/headlines/y2006/06nov_loworbit.htm, (last date accessed: 7 Jan. 2007)

Deleted: uary

Campbell, B. A., Campbell, D. B. and Nolan, M. 2003. New High-Resolution 70-cm Wavelength Radar Images of the Moon. *34th Annual Lunar and Planetary Science Conference, March 17-21, 2003, League City, Texas*. Abstract No.1700. ([NASA/ADS](#))

Campbell, B. A., Campbell, D. B., Hawke, B. R. and Lucey, P. G. 2004. Radar Properties of Lunar Basin Deposits. *35th Lunar and Planetary Science Conference, March 15-19, 2004, League City, Texas*. Abstract No. 1659. ([NASA/ADS](#))

Campbell, B. A., Campbell, D. B. and Chandler, J. 2005. New 70-cm Radar Mapping of the Moon. *36th Annual Lunar and Planetary Science Conference, March 14-18, 2005, in League City, Texas*. Abstract No.1385. ([NASA/ADS](#))

Campbell, B. A., Carter, L. M., Campbell, D. B., Hawke, B. R., Ghent, R. R. and Margot, J. L. 2006. *37th Annual Lunar and Planetary Science Conference, March 13-17, 2006, League City, Texas*, Abstract No. 1717. ([NASA/ADS](#))

Campbell, D.B., Campbell, B.A., Carter, L.M., Margot, J.L. and Stacy, N.J.S. 2006. *Nature*. 443(7113):835-837. ([NASA/ADS](#))

Campbell, D.B and Carter, L.M. 2006. Earth Based Radar Imagery and Topography: Input to LCross Target Selection. URL: www.lpi.usra.edu/meetings/lcross2006/pdf/9002.pdf, (last date accessed: 7 Jan. 2007)

Deleted: uary

Carlotto, M.J. 1996. Shape from Shading. URL:
<http://www.newfrontiersinscience.com/martianenigmas/Articles/SFS/sfs.html>, (last date
accessed: 19 Feb. 2007)

Cherrington, E.H. 1984 (2d). *Exploring the Moon through Binoculars and Small Telescopes*.
Dover.

Chevrel, S. and Legrand, M. 1994. Determining Heights. Section 4.5.2.2, Chap. 5, Vol 1. In
Martinez, Patrick (ed). *The Observer's Guide to Astronomy*. Cambridge Univ. Press, New York
City, New York. pp. 144-153 ([NASA/ADS](#))

Chin, G., Bartels, A., Brylow, M., Foote, M., Garvin, J., Kaspar, J., Keller, J., Mitrofanov, I.,
Raney, K. and Robinson, M. et al. 2007. Update on the Lunar Reconnaissance Orbiter: The
Instrument Suite and Mission. *38th Annual Lunar and Planetary Science Conference, March
12-16, 2007, League City, Texas*, Abstract No. 1764. URL:
<http://www.lpi.usra.edu/meetings/lpsc2007/pdf/1764.pdf> (last date accessed: 7 Feb. 2007)

Cook, A. C., Robinson, M. S. and Watters, T. R. 2000. Planet-wide Lunar Digital Elevation
Model. *31st Annual Lunar and Planetary Science Conference, March 13-17, 2000, Houston,
Texas*. Abstract No. 1978. ([NASA/ADS](#))

Cook, A. C., Spudis, P. D., Robinson, M. S., and Watters, T. R. 2002. Lunar Topography and
Basins Mapped Using a Clementine Stereo Digital Elevation Model. *33rd Annual Lunar and
Planetary Science Conference, March 11-15, 2002*. Abstract No. 1281. ([NASA/ADS](#))

Davies, M.E., Colvin, T.R., Meyer, D.L. and Nelson, S. 1994a. The Unified Lunar Control Network: 1994 Version. *J. Geophysical Res.* 99(E11):23,211-23,214 ([NASA/ADS](#))

Davies, M.E., Colvin, T.R., Meyer, D.L. and Nelson, S. 1994b. The Unified Lunar Control Network: 1994 Version. (Datafile). URL: http://astrogeology.usgs.gov/Projects/LunarConsortium/data/topo_con/control.asc, (last date accessed: 7 Jan. 2007)

Deleted: uary

Davis III, W.F. 1997. Determination of Lunar Elevations by the Shadow Method: Analysis and Improvements. URL: <http://www.zone-vx.com/vertical-studies.pdf>, (last date accessed: 7 Jan. 2007).

Deleted: uary

Davis III, W.F. 1998. The Mountains of the Moon. *Sky & Telescope*. 96(5):114-118.

Elachi, C., Kobrick, M., Roth, L., Tiernan, M. and Brown, W. E., Jr. 1976. Local lunar topography from the Apollo 17 ALSE radar imagery and altimetry. *The Moon*. 15:119-131. ([NASA/ADS](#))

Ellison, D. Oct. 2, 2006. The Big Guns. URL: <http://www.planetary.org/blog/article/00000710/>,
(last date accessed: 7 Jan. 2007).

Deleted: uary

Evans, R. June 2006a. The Moon on a Spreadsheet: Photoclinometry using Excel. *Selenogology Today*. 1:21-59 ([Link](#))

Field Code Changed

Evans, R. June 2006b. *Excel Spreadsheets for SFS Photoclinometry*. URL:
<http://digilander.libero.it/qlrgroup/workbooks.zip>. (last date accessed: 17 Feb. 2007)

Gaddis, L. R., Skinner, J. A., Jr., Hare, T., Tanaka, K., Hawke, B. R., Spudis, P., Bussey, B.,
Pieters, C., and Lawrence, D. 2006. The Lunar Geologic Mapping Program and Status of
Copernicus Quadrangle Mapping. *37th Annual Lunar and Planetary Science Conference, March*
13-17, 2006, League City, Texas, Abstract No. 2135. ([NASA/ADS](#))

Griffin, M. (NASA). Oct. 3, 2006. Administrator's Remarks Before the 57th Annual
International Astronautical Congress. URL:
http://www.nasa.gov/pdf/159915main_IAC_Valencia%20-2006.pdf, (last date accessed: 7 Jan.
2007).

Deleted: uary

Hale, W.S. and Head, J. W. 1979. Central Peaks in Lunar Craters: Morphology and Morphometry. *Lunar and Planetary Science X*, Proceedings. pp. 491-493. ([NASA/ADS](#))

Hale, W.S. and Grieve, R.A. F. 1982. Central Peak and Peak Ring Development: Constraints from Lunar Peak Volumes. *Lunar and Planetary Science XIII*, Proceedings. pp. 297-298. ([NASA/ADS](#))

[Hapke, B. 1993. *Theory of reflectance and emittance spectroscopy*. Cambridge Univ. Press, Cambridge, UK.](#)

Heiken, G.H., Vaniman, D.T. and French, B.M. 1991. *Lunar Sourcebook - A User's Guide to the Moon*. Cambridge Univ. Press. Cambridge, England. Table 4.1. ([Link](#))

Hiesinger, H. and Head III, J.W. 2006. New Views in Lunar Geoscience: An Introduction and Overview. In Jolliff, B.L. et al (eds). New Views of the Moon. *Reviews in Mineralogy & Geochemistry*. 60:1-81.

Honda, C., Morota, T., Yokota, Y., Haruyama, J., Ohtake, M., Matsunaga, T., Ogawa, Y., Demura, H., Hirata, N., Iwasaki, A., *et al.* 2007. Preliminary Test of Accuracy of Digital Terrain Model Derived from Selene/LISM/TC Data. *38th Annual Lunar and Planetary Science Conference, March 12-16, 2007, League City, Texas*, Abstract No. 1899. URL: <http://www.lpi.usra.edu/meetings/lpsc2007/pdf/1899.pdf> (last date accessed 7 Feb. 2007)

Jamieson, H.D. 1993. The Lunar Dome Survey - Fall, 1992 progress report. *J.A.L.P.O.* 37(1):14-17. ([NASA/ADS](#))

Jamieson, H.D. 1997. Lunar Observer's Toolkit. URL:

<http://www.glrgroup.org/download/tool.exe>, (last date accessed: 7 Jan. 2007).

Deleted: uary

Jet Propulsion Laboratory. 2006. Biography of Dr. Charles Elachi, Director of JPL. URL:

<http://www.jpl.nasa.gov/bios/elachi/>, (last date accessed 7 Jan. 2007).

Deleted: uary

Kapral, C.A. and Garfinkle, R.A. 2005. GLR Lunar Domes Catalog, URL:

<http://www.glrgroup.org/domes/kapralcatalog.htm>, (last date accessed: 7 Jan. 2007).

Deleted: uary

Kirk, R.L., Barrett, J.N. and Soderblom, L.A. 2003. Photoclinometry Made Simple ?
Proceedings of the Conf. on Advances in Planetary Mapping, Houston, Texas, 2003. URL:
http://astrogeology.usgs.gov/Projects/ISPRS/MEETINGS/Houston2003/abstracts/Kirk_isprs_mar03.pdf, (last date accessed: 19 Feb. 2007)

Konopliv, A. S., Binder, A. B., Hood, L. L., Kucinskis, A. B., Sjogren, W. L. and Williams, J. G. 1998. Improved Gravity Field of the Moon from Lunar Prospector. *Science*. 281(5382): 1476. ([NASA/ADS](#))

Kopal, Z. 1962. Determination of Altitudes on the Moon. Part IV in Topography of the Moon. Chap. 7 in Kopal, Z. (ed). *Physics and Astronomy of the Moon*. Academic Press, New York, N.Y. ([NASA/ADS](#))

Koschny, D., Foing, B.H., Frew, D., Almeida, M., Sarkarati, M., Volp, J., Grande, M., Huovelin, J., Josset, J. L., Nathues, A. *et al.* 2007. SMART-1 Lunar Science Planning. *38th Annual Lunar and Planetary Science Conference, March 12-16, 2007, League City, Texas*, Abstract No. 1996. URL: <http://www.lpi.usra.edu/meetings/lpsc2007/pdf/1996.pdf> (last date accessed 7 Feb. 2007)

Kuiper, G.P. 1960. *Photographic Lunar Atlas*. Univ. of Chicago, Chicago, Illinois.

([NASA/ADS](#))

Kuiper, G.P. 1961. *Orthographic Atlas of the Moon*. Univ. of Ariz. Press, Tuscon, Arizona.

([NASA/ADS](#))

Law, N. M., Mackay, C. D. and Baldwin, J. E. 2006. Lucky Imaging: High Angular Resolution Imaging in the Visible from the Ground. *Astro. & Astrophysics*. 446(2):739-745. ([NASA/ADS](#))

Lemoine, F.G., Smith, D.E., Zuber, M.T., Neumann, G.A., and Rowlands, D.D. 1997. A 70th Degree Lunar Gravity Model (GLGM-2) from Clementine and other tracking data. *J. Geo. Res.* 102:16, 339-359. ([NASA/ADS](#))

Lena, R. 2006. Editorial. *Selenology Today*. 1:3-4 ([Link](#))

Lena, R., Pau, K.C., Phillips, J., Fattinnanzi, C., and Wöhler, C. 2006. Lunar Domes: A Generic Classification of the Dome near Valentine, Located at 10.26 E and 31.89 N. *JBAA*. 116(1):34-

39. URL: <http://www.glrgroup.org/domes/File0351/File0351.pdf>, (last ~~date~~ accessed 12 Feb. 2007) ([NASA/ADS](#))

Deleted: date

Lena, R., Wöhler, C., Bregante M.T., and Fattinanzi, C. 2006. A Combined Morphometric and Spectrophotometric Study of the Complex Lunar Volcanic Region in the south of Petavius.

JRASC. 100(1): 14-24. URL: http://www.christian-woehler.de/petavius_jrasc.pdf, (last accessed 12 Feb. 2007) ([NASA/ADS](#))

Deleted: date

Deleted: date

Lena, R., Wöhler, C., Bregante, M. T., Phillips, J. , Zompatori, D., and Sbarufatti, G. 2007.

Two Domes in Mare Fecunditatis near Messier Crater. *Selenology Today.* 3:25-37. URL:

<http://digidownload.libero.it/glrgroup/selenologytoday3.pdf>, (last date accessed 12 Feb. 2007)

Deleted: date

MacDonald, T.L. 1931. On the Determination of Relative Lunar Altitudes. *J.B.A.A.* 41:267-379.

Margot, J.L., Campbell, D.B., Jurgens, R.F., and Slade, M.A. 1999a. The Topography of Tycho Crater. *J. Geo. Res.* 104(E5):11875-11882. ([NASA/ADS](#))

Margot, J. L., Campbell, D. B., Jurgens, R. F., Slade, M. A. 1999b. Topography of the Lunar Poles from Radar Interferometry: A Survey of Cold Trap Locations. *Science.* 284(5420):1658-1660. ([NASA/ADS](#))

Margot, J.L., Campbell, D.B., Jurgens, R.F. and Slade, M.A. 2000. Digital Elevation Models of the Moon from Earth-Based Radar Interferometry. *IEEE Trans. on Geoscience and Remote Sensing*. 38(2):1122-1133 ([Link](#))

McDowell, J. 2004. Lunar Nomenclature. URL: <http://host.planet4589.org/astro/lunar/>, (last date accessed 7 Jan. 2007).

Deleted: uary

Mosher, J. and Bondo, H. 2006. Lunar Terminator Visualization Tool (LTVT) (software) URL: http://inet.uni2.dk/~d120588/henrik/jim_lTVT.html, (last date accessed 7 Jan. 2007).

Deleted: uary

NASA. 1980. Lunar Topographic Orthophotomap (LTO) Series Apollo Photo and Map Index Map. URL: <http://www.lpi.usra.edu/resources/mapcatalog/LTO/references.html>, (last date accessed: 7 Jan. 2007).

Deleted: uary

NASA. 2006a. Clementine Base Map Image Collections CL-3001 to CL-3015. URL: http://pds-imaging.jpl.nasa.gov/Admin/resources/cd_clementine.html#clmBASE, (last date accessed: 7 Jan. 2007).

Deleted: uary

NASA. 2006b. Clementine HiRes Image Collections CL-4001 to CL-4078. URL: http://pds-imaging.jpl.nasa.gov/Admin/resources/cd_clementine.html#clmUVVIS, (last date accessed: 7 Jan, 2007).

Deleted: uary

NASA. 2006c. Clementine Polar HiRes Image Collections CL-6001 to CL-6022. URL: http://pds-imaging.jpl.nasa.gov/Admin/resources/cd_clementine.html#clmHIRES, (last date accessed: 7 Jan, 2007).

Deleted: uary

NASA. 2006d. NASA and Google to Bring Space Exploration Down to Earth. NASA Press Release 06_96AR. URL: http://www.nasa.gov/centers/ames/news/releases/2006/06_96AR.html, (last date accessed: 7 Jan, 2007).

Deleted: uary

NASA and JPL. 2006. Planetary Data Systems Viewer Software Download Webpage. URL: http://pds.jpl.nasa.gov/tools/software_download.cfm, (last date accessed: 7 Jan, 2007).

Deleted: uary

NASA and Washington Univ. in St. Louis. 2006a. Clementine Gravity and Topography Data Archive. Planetary Data Service Geosciences Node. (GLTM-2B digital elevation model). URL: <http://pds-geosciences.wustl.edu/missions/clementine/gravtopo.html>, (last date accessed: 7 Jan, 2007).

Deleted: uary

NASA and Washington Univ. in St. Louis. 2006b. PDS Clementine Data Archive. Planetary Data Service Geosciences Node. URL: [http://pds-](http://pds-geosciences.wustl.edu/missions/clementine/index.htm)

[geosciences.wustl.edu/missions/clementine/index.htm](http://pds-geosciences.wustl.edu/missions/clementine/index.htm), (last date accessed: 7 Jan 2007).

Deleted: uary

Pike, R. J. 1976. Crater dimensions from Apollo data and supplemental sources. *The Moon*. 15:463-477. ([NASA/ADS](#))

Pike, R. J. 1977. Apparent depth/apparent diameter relation for lunar craters. *Lunar Sci. Conf., VIII, March 14-18, 1977, Proceedings. (Vol. 3)*. ([NASA/ADS](#))

Rosiek, M. R., Archinal, B. A., Kirk, R. L., Becker, T. L., Weller, L., Redding, B., Howington-Kraus, E. and Galuszka, D. 2006. Utilization of Digitized Apollo and Lunar Orbiter Imagery for Mapping the Moon. *37th Annual Lunar and Planetary Science Conference, March 13-17, 2006, League City, Texas*, Abstract No. 2171. ([NASA/ADS](#))

Rosiek, M.R., Cook, A.C., Robinson, M.S., Watters, T.R., Archinal, B.A., Kirk, R.L., and Barrett, J.M. 2007. A Revised Planet-Wide Digital Elevation Model of the Moon. *38th Annual Lunar and Planetary Science Conference, March 12-16, 2007, League City, Texas*, Abstract No. 2297. URL: <http://www.lpi.usra.edu/meetings/lpsc2007/pdf/2297.pdf> (last date accessed 7 Feb. 2007)

Rosiek, M.R., Kirk, R. and Howington-Kraus, E. 2001. Combining Lunar Photogrammetric Topographic Data with Clementine LIDAR data. URL: http://astrogeology.usgs.gov/Projects/ISPRS/MEETINGS/Flagstaff2001/abstracts/isprs_etm_OC_T01_rosiek_moon_topography.pdf, (last date accessed: 7 Jan. 2007).

Deleted: uary

Rosiek, M. R., Kirk, R., and Howington-Kraus, E. 2002. Color-coded Topography and Shaded Relief Maps of the Lunar Hemispheres. *33rd Annual Lunar and Planetary Science Conference, March 11-15, 2002*. Abstract No. 1792. ([NASA/ADS](#))

Shaw, Brenden, GLR Group. 2006. Lunar Dome Maps. URL: <http://www.glrgroup.org/domes/domeatlas.htm>, (last date accessed 12 Feb. 2007).

Deleted: ruary

Smith, D.E., Zuber, M.T., Neumann, G.A. and Lemoine, F.G. 1997. Topography of the Moon from the Clementine LIDAR. *J. Geo. Res.* 102:1591. ([NASA/ADS](#))

St. Clair, J. H., Carder, R. W., and Schirmerman, L. A. 1979. United States Lunar Mapping - A Basis for and Result of Project Apollo. *Moon and the Planets.* 20:127-148. ([NASA/ADS](#))

Schirmerman, L., U.S. Defense Mapping Agency. 1973. The Lunar Cartographic Dossier. NASA Pub. NASA-CR 1464000. URL:

http://www.lpi.usra.edu/resources/mapcatalog/LTO/lto_references.pdf, (last date accessed: 7 Jan. 2007).

Deleted: uary

Stacy, N. J. S., Campbell, D. B. and Ford, P. G. 1997. Arecibo radar mapping of the lunar poles: A search for ice deposits. *Science.* 276:1527-1530. ([NASA/ADS](#))

Thompson, T. W. 1979. A Review of Earth-based Radar Mapping of the Moon. *Moon and the Planets.* 20:179-198. ([NASA/ADS](#))

Tubbs, R. N. 2004. Lucky Exposures: Diffraction-Limited Astronomical Imaging through the Atmosphere. Ph.D dissertation. *The Observatory.* 124:159-160. ([NASA/ADS](#))

U.S. Air Force, NASA and Aeronautical Chart and Information Center. 1967. (1st Ed.) *Lunar Aeronautical Chart 112: Tycho*. ([Link](#))

U.S. Defense Mapping Agency. 197_. NASA Lunar Topophotomap (TPM) series. URL: <http://www.lpi.usra.edu/resources/mapcatalog/topophoto/>, (last date accessed: 7 Jan., 2007).

Deleted: uary

U.S. Defense Mapping Agency. 1974. NASA Lunar Topophotomap 41B4S1(50): [Apollo 15 Landing Area](#). URL: <http://www.lpi.usra.edu/resources/mapcatalog/topophoto/41B4S1/>, (last date accessed: 7 Jan., 2007).

Deleted:).

Deleted: uary

U.S. Defense Mapping Agency. 1974-1976. NASA Lunar Topographic Orthophotomap (LTO) Series Map. URL: <http://www.lpi.usra.edu/resources/mapcatalog/LTO/>, (last date accessed: 7 Jan., 2007).

Deleted: uary

U.S. Defense Mapping Agency. 1975a. NASA Lunar Topographic Orthophotomap LTO-41B4: [Hadley](#). URL: http://www.lpi.usra.edu/resources/mapcatalog/LTO/lto41b4_2/, (last date accessed: 7 Jan., 2007).

Deleted: uary

U.S. Geological Survey (USGS). 2002. Lunar Clementine Globe (Petal Leaf Map). URL:
<http://astrogeology.usgs.gov/Gallery/MapsAndGlobes/moon.html#Globes>, (last date accessed: 7
Jan. 2007)

Deleted: uary

USGS. 2003. Color-Coded Topography and Shaded Relief Map of the Lunar Near Side and Far
Side Hemispheres. Geologic Investigations Map Series I-2769. URL:
<http://geopubs.wr.usgs.gov/i-map/i2769/>, (last date accessed: 7 Jan. 2007)

Deleted: uary

USGS. 2006a. Clementine Map of the Topography of the Moon. In *The Clementine Mission*.
URL: <http://astrogeology.usgs.gov/Projects/Clementine/>, (last date accessed: 7 Jan. 2007)

Deleted: uary

USGS. 2006b. Gazetteer of Planetary Nomenclature. URL:
[http://planetarynames.wr.usgs.gov/jsp/FeatureTypes2.jsp?system=Earth&body=Moon&systemI
D=3&bodyID=11](http://planetarynames.wr.usgs.gov/jsp/FeatureTypes2.jsp?system=Earth&body=Moon&systemID=3&bodyID=11), (last date accessed 7 Jan. 2007).

Deleted: uary

USGS. 2006c. Lunar Control Networks. URL:
<http://astrogeology.usgs.gov/Projects/ControlNetworks/Moon/>, (last date accessed 7 Jan. 2007).

Deleted: uary

USGS. 2006d. PDS Map-A-Planet Help Page: Data Sets. URL:
http://pdsmaps.wr.usgs.gov/PDS/public/explorer/html/data_set.htm, (last date accessed 7 Jan.
2007).

Deleted: uary

USGS. 2006e. Planetary Data Services Map-A-Planet Online Application: Moon. URL:

<http://pdsmaps.wr.usgs.gov/PDS/public/explorer/html/moonpick.htm>, (last date accessed 7 Jan. 2007).

Deleted: uary

USGS. 2006f. USGS Digital Data Viewer: dlgy32 Pro. (Software download website). URL:

<http://mcmweb.er.usgs.gov/drc/dlgy32pro/>, (last date accessed 3 Feb. 2007)

Deleted: date

USGS. 2007. ISIS: Integrated Software for Imagers and Spectrometers. URL:

<http://isis.astrogeology.usgs.gov/>, (last date accessed 19 Feb. 2007)

USGS, NASA and US Airforce ACIC. 197_. A Geologic Atlas of the Moon. URL:

<http://www.lpi.usra.edu/resources/mapcatalog/usgs/>, (last date accessed 7 Jan. 2007).

Deleted: uary

Viscardy, Georges. 1985. *Atlas-guide photographique de la lune: ouvrage de référence à haute résolution*. Masson.

Whitaker, E. A., Kuiper, G. P., and Hartmann, W. K. 1963. *Rectified Lunar Atlas*. Univ. of Ariz. Press. ([NASA/ADS](#))

Westfall, John E. 2000. *Atlas of the Lunar Terminator*. Cambridge Univ. Press.

Wöhler, C. and Hafezi, K. 2005. A General Framework for Three-Dimensional Surface Reconstruction by Self-Consistent Fusion of Shading and Shadow Features. *Pattern Recognition*. 38(7):965-983. URL: http://www.christian-woehler.de/woehler_hafezi_patrec.pdf,
(last ~~date~~ accessed 12 Feb. 2007)

Deleted: date

Wöhler, C., Lena, R. , Lazzarotti, P. , Phillips, J. , Wirths, M. and Pujic, Z. 2006. A Combined Spectrophotometric and Morphometric Study of the Lunar Mare Dome Fields Near Cauchy, Arago, Hortensius, and Milichius. *Icarus*. 183(2):237-264. URL: http://www.christian-woehler.de/lunar_domes_spectrophot_morph_icarus.pdf, (last ~~date~~ accessed 12 Feb. 2007)
([NASA/ADS](#))

Deleted: date

Wöhler, C., Lena, R., Phillips, J., Bregante, M.T., Lazzarotti, P. and Sbarufatti, G. 2007. Vertical Studies about Rupes Bûrg. *Selenology Today*. 3:65-78 ([Link](#))

Wood, C. A. 1973. Central Peak Heights and Crater Origins. *Icarus*. 20:503. ([NASA/ADS](#))

Wood, C.A. and Andersson, L.A. 1974. Lunar crater statistics - Earth face. (Unpublished).

Wood, C.A. 13 May 2004. A New/Old Catalog of Lunar Craters. *Lunar Picture of the Day* (LPOD). URL: <http://www.lpod.org/archive/archive/2004/05/LPOD-2004-05-13.htm>, (last date accessed 7 Jan. 2007).

Deleted: uary

Wood, C.A. 24 Dec. 2006. Measuring a Serpent. *Lunar Picture of the Day*. URL: <http://www.lpod.org/?m=20061224>, (last date accessed 7 Jan. 2007).

Formatted: Font: Italic

Deleted: uary

Wood, C.A. and Andersson, L. 1978. New Morphometric Data for Fresh Lunar Craters. *Lunar and Planetary Science Conference, 9th, Houston, Tex., March 13-17, 1978, Proceedings*. New York, Pergamon Press, Inc., 1978, p. 3669-3689. ([NASA/ADS](#))

Yokota, Y., Haruyama, J., Ohtake, M., Matsunaga, T., Honda, C., Morota, T., Demura, H., Nirata, N. and LISM Working Group. 2007. Kilometer scale roughness analysis of lunar digital terrain model. *38th Annual Lunar and Planetary Science Conference, March 12-16, 2007, League City, Texas*, Abstract No. 2430. URL: <http://www.lpi.usra.edu/meetings/lpsc2007/pdf/2430.pdf> (last date accessed 7 Feb. 2007)

Zuber, M. T., Smith, D. E., Lemoine, F. G. and Neumann, G. A. 1994. The Shape and Internal Structure of the Moon from the Clementine Mission. *Science*. 266(5192):1839-1843.

([NASA/ADS](#))

Appendix – Description of Apollo era crater table digitization

A table craters and satellite feature names, positions and diameters was prepared from the online USGS Gazetteer of Planetary Nomenclature. [Pike 1976](#) was reviewed. Where Pike's measurement corresponded to (1) the Gazetteer feature name and (2) the crater diameter was within 3 kilometers of the Gazetteer measurement, Pike's crater diameter, depth and peak height were digitized. Approximately 239 crater depths were digitized. [Arthur 1974](#) was reviewed. Where Arthur's measurement corresponded to (1) the Gazetteer feature name and (2) the crater diameter was within 5 kilometers of the Gazetteer measurement, Arthur's crater diameter was digitized. Eleven craters from [Elachi et al. 1976](#) and one measurement from [Margot et al. 1999a](#) were added. 37 central peak measurements from [Wood 1973](#) were added.

This resulted in a table pairing the USGS Gazetteer lunar feature name, position, NCLN crater diameter with the crater diameter and depth from other higher accuracy Apollo era catalogue sources.

Next the initial digitization was filtered to exclude craters larger than 10 km in diameter where the diameter varied by more than 10% from the [NCLN](#) crater diameter.

The difference between the [NCLN](#) crater diameter and source catalogue diameters was computed (except for the list of central peaks from [Wood 1973](#)) in order to verify an association based on feature name and size. For craters over 10 kilometers in diameter, the criteria of a 10% difference was applied. For craters less than 10 kilometers in diameter, all craters were included because a criterion based on crater diameter difference was not statistically meaningful due to the whole number precision used in the GPN catalogue. The filter criteria excluded the measurement of Tycho from [Margot *et al.* 1999a](#).

In the final table, 91% of the craters have a diameter that differs from the GPN measurement by one kilometer or less. Examples of craters that meet the 10% difference criterion and also that have absolute crater diameter differences exceeding 10 kilometers are larger named craters such as Clavius, Hipparchus, Langrenus and Neper.

In the final table, 86% of craters have a diameter less than 20km, 11% between 20km and 50km, and 3% are larger than 50km in diameter. 50% have depths of less than 1km, 33% between 1 and 2km, 12% between 2 and 3km, and 4% greater than 3km.